Rapid Climate Oscillations in the Northeast Pacific During the Last Deglaciation Reflect Northern and Southern Hemisphere Sources

Alan C. Mix[1], David C. Lund[2], Nicklas G. Pisias[1], Per Bodén[3],
Lennart Bornmalm[4], Mitch Lyle[5], and Jennifer Pike[6]

Planktic foraminiferal species abundances, benthic and planktic foraminiferal stable isotopes, radiocarbon, and organic carbon contents of deep-sea cores off Oregon and Northern California reveal abrupt millennial-scale climate oscillations during the past 20,000 years. Changes in the near-surface ocean are essentially coincident with the Bølling-Allerød and Younger-Dryas climate oscillations observed in Greenland ice cores and North Atlantic sediments. This finding supports the concept of atmospheric transmission of climate signals between oceans within the Northern Hemisphere. Abrupt cooling of North Pacific surface waters occurred in mid-Holocene time, indicating that the warm events of the early Holocene and deglaciation are anomalous relative to modern climate. Higher export productivity is associated with warm events in the North Pacific. These biotic changes may have contributed to variations in the shallow (~400 m depth) oxygen minimum zone off California, and may in part explain the apparent coincidence of local anoxia with warming in Greenland. Benthic foraminiferal $\delta^{13}C$ and ^{14}C data from lower intermediate waters (980 m depth) suggests that higher ventilation (either faster formation or greater gas exchange) occurred during the Bølling-Allerød and early Holocene warm events. Synchronicity with surface ocean changes points to North Pacific source waters, and ventilation during warming leads to a hypothesis that salinity rather than temperature controls intermediate water formation at these times. In the deep North Pacific (2700 m depth) benthic foraminiferal $\delta^{18}O$ changes imply early warming roughly synchronous with warming of the Southern Ocean. Both $\delta^{13}C$

[1]College of Oceanic and Atmospheric Sciences, Oregon State University, Corvallis, Oregon
[2]Kennedy School of Government, Harvard University, Cambridge, Massachusetts
[3]Department of Geology and Geochemistry, Stockholm University, Stockholm, Sweden
[4]Department of Marine Geology, University of Goteborg, Goteborg, Sweden
[5]Center for Geophysical Investigation of the Shallow Subsurface, Boise State University, Boise, Idaho
[6]Department of Earth Sciences, University of Cardiff, Cardiff, Wales

and ^{14}C suggest an abyssal ventilation event (either faster formation or greater gas exchange) during deglaciation at the same time as short-term cooling in Antarctica, pointing to a Southern Ocean source of variability in the deep Pacific. Thus, climate changes that characterize both northern and southern sources appear to propagate through the Pacific Ocean.

1. INTRODUCTION

Understanding climate variability on millennial time scales has become a major focus of the paleoclimate community. Starting in the 1970's, ice-core records clearly demonstrate variability on millennial time scales [*Dansgaard, et al.,* 1971]. Frequencies of variation similar to the ice core records were first documented in the North Atlantic by *Pisias et al.* [1973]. Major episodes of ice rafting, the so-called Heinrich events, have been documented in the North Atlantic [*Bond et al.,* 1993; *Bond and Lotti,* 1995] and may represent dramatic surges of former ice streams [*MacAyeal,* 1993]. These events are part of a package of high-frequency variations of climate in the North Atlantic and adjacent regions including deep-water circulation [*Oppo and Lehman,* 1995].

Recent evidence from both land and sea indicates that the climate of some regions outside of the North Atlantic also varied at millennial scales [*Porter and An,* 1995; *Thunell and Mortyn,* 1995; *Kotilainen and Shackleton,* 1995; *Kennett and Ingram,* 1995; *Lowell et al.,* 1995; *Charles et al.,* 1996; *Curry and Oppo,* 1997; *van Geen et al.,* 1997; *Lund and Mix,* 1998]. The potential exists for a widespread response to global forcing external to the climate system [*Broecker,* 1995], for a response arising within the climate system of the North Atlantic region and propagating elsewhere [*Clark and Bartlein,* 1995], or for an effect elsewhere within the climate system that is independent of North Atlantic variability.

The challenge now is to assess how millennial-scale events, reasonably well known in the North Atlantic record, are related to events identified globally, and more importantly to identify the processes that provide global linkage on these time scales. Are the linkages made through the atmosphere, the deep and surface ocean, or both? Does the rest of the world follow changes initiated in the North Atlantic, or does the chain of events start elsewhere?

Our strategy is to identify the timing of regional responses that yield insight into the dynamics of rapid climate changes. This approach follows that of establishing the phase sequence of regional paleoclimatic oscillations on longer (orbital) scales [*Imbrie et al.,* 1989]. Resolving sequences of events on the short timescales examined here presents special challenges, however, as it pushes the limits of chronologic uncertainty. We approach this uncertainty in two ways. First, we focus on an age range that can be dated precisely by radiocarbon, specifically on short-term climatic events of the last deglaciation as examples of millennial scale changes. Here we follow *Alley and Clark* [1999], who summarize current knowledge of the global distribution of such events and highlight the need for new data from poorly known areas such as the North Pacific. Second, we examine relationships between multiple proxies of different climatic systems within the same core samples. Leads or lags among such proxies within the same samples are reliable, even if the absolute chronology is uncertain.

2. WHY THE NORTHEAST PACIFIC?

Sediments from the Santa Barbara Basin off southern California and the Gulf of California already provide clear evidence of millennial-scale events in the shallow reaches of the Pacific Ocean. The patterns of change are remarkably similar to those of the North Atlantic and in Greenland ice cores [*Keigwin and Jones,* 1990; *Behl and Kennett,* 1996; *Cannariato et al.,* 1999; *Hendy and Kennett,* 1999], but the precise timing of events and processes driving such changes remain unclear.

Increases in the oxygen content of bottom waters of the Santa Barbara Basin appear to be associated with cool events in Greenland ice cores and North Atlantic sediments [*Behl and Kennett,* 1996; *Cannariato et al.,* 1999]. Plausible mechanisms to explain variations in oxygen here include changing ventilation of the North Pacific thermocline, shifts in intermediate water masses, and changes in large-scale biological productivity of the Pacific that modify the region's oxygen minimum zone [*Kennett and Ingram,* 1995].

Here, we examine variability of surface and deep waters and evidence for paleoproductivity in cores off Oregon and Northern California (Figure 1). This area is important for several reasons. Sediment cores here monitor: 1) the wind-driven position of the boundary between the subtropical and subpolar gyres of the North Pacific as reflected in the character of the California Current [*Lynn and Simpson,* 1987], 2) upwelling in a highly productive eastern boundary current in a region where much of the flux of organic matter to the deep North Pacific occurs [*Huyer,* 1983], and 3) lower intermediate and deep waters of the North Pacific, where world's "oldest", most nutrient-rich, and lowest $\delta^{13}C$ deep waters (i.e., those longest isolated from interaction with the sea surface) are found [*Reid,* 1965; *Mantyla and Reid,* 1983; *Broecker et al.,* 1985].

High hemipelagic sedimentation rates at two sites off Northern California and Southern Oregon, driven by rapid erosion of the continent and high biogenic productivity, facilitate high-resolution study of climate change. These

two sites are particularly well placed for monitoring the upper and lower bounds of nutrient-rich North Pacific Deep Water (Figure 2). Core W8709A-13PC (42.117°N, 125.750°W, 2712 m water depth) lies within the gradient between low-δ^{13}C Pacific Deep Water and higher-δ^{13}C bottom waters that enter the Pacific basin from the south [*Kroopnick, 1985*]. Ocean Drilling Program (ODP) Site 1019 (41.682°N, 124.930°W, 980 m water depth) monitors the gradients above Pacific Deep Water where it mixes with overlying intermediate waters.

Stable isotope data from core W8709A-13PC were documented previously [*Lund and Mix, 1998*] but nine new radiocarbon dates reported here improve the chronology. This site, located 130 km from the Oregon coast, is under the advective core of the California Current outside of the coastal upwelling system. Planktonic foraminifera here record the strength and character of eastern boundary advection related to the position of the North Pacific Subpolar Front (Figure 2).

ODP Site 1019, 70 km offshore of Eureka, California, records upper-ocean variability and export productivity within the wind-driven coastal upwelling system. Because of its proximity to the coast, it has high sedimentation rates (averaging >50 cm/ka during the last deglaciation) and thus offers a highly detailed record of millennial-scale events during the last glacial cycle [*Lyle et al., 1997*].

Figure 1. Core W8709A-13PC and ODP Site 1019 are under the northern California Current, south of the North Pacific Subpolar Front. Upper ocean proxies here are sensitive to both the position of the Subpolar Front and the heat content of the northern subtropical gyre. Site 1019 is under the coastal upwelling system, while W8709A-13PC is under the advective core of the California Current. Here, AC is the Alaska Current, and CC is the California Current.

3. HYPOTHESES

We explore several working hypotheses to explain millennial-scale climate oscillations observed in Pacific sediments, considering effects of upper ocean circulation and temperature, influences of biological productivity on the properties of thermocline and intermediate waters, and varying sources of mid-depth and deep water masses.

3.1. Upper Ocean Circulation and Temperature

Model studies suggest that atmospheric transmission of North Atlantic cooling to the North Pacific could be significant and rapid [*Manabe and Stouffer, 1988; Mikolajewicz et al., 1997*]. A first working hypothesis based on such models is that changes in sea-surface temperatures of the North Pacific would be similar to those of the North Atlantic.

To test this hypothesis, we examine the timing of upper ocean circulation changes in the northeast Pacific. If changes in upper ocean temperatures or circulation in the North Pacific mimic those of the North Atlantic, perhaps with a small lag, then atmospheric transmission of a regional cooling is likely. *Hendy and Kennett* [1999] argue for such a connection based on variations in surface water conditions in Santa Barbara Basin.

If the North Pacific surface ocean record is substantially different from that of the North Atlantic, then other processes may be important. For example, a modeling
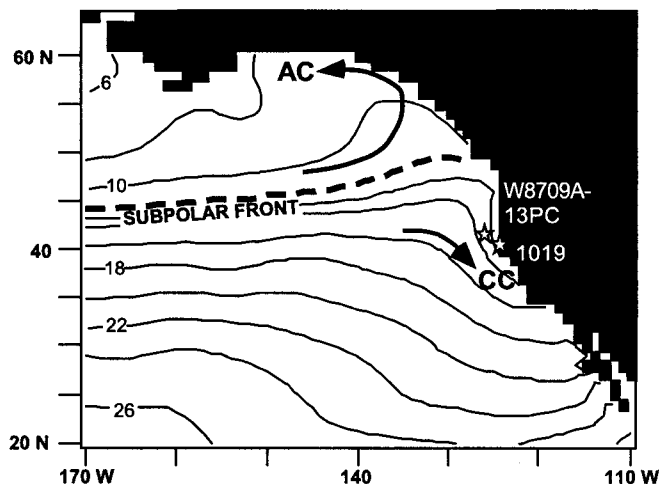
study that includes the hypothesized effect of rapid reduction of Laurentide Ice Sheet elevation during Heinrich events predicts cooling in western North America at the same time as warming of the North Atlantic [*Hostetler et al., 1999*].

3.2. North Pacific Intermediate Water

Cooling in the North Pacific has the potential to modify formation of North Pacific Intermediate Water (NPIW). At present, little or no deep water forms and intermediate water formation is limited in the North Pacific because the surface ocean here has relatively low salinity [*Warren, 1983*]. Salinity is low because evaporation rates are low. Evaporation rates are low because the sea surface is cool. To some extent, the sea surface is cool because there is little formation of intermediate or deep water, which would draw oceanic heat poleward from the subtropics. This loop of cause and effect suggests the possibility of dramatic change into a state with greater formation of intermediate or deep water which could be self sustaining, if first initiated by either extreme cooling or higher sea-surface salinity.

NPIW forms today in the Northwest Pacific and in the Sea of Okhotsk due to extreme cooling of the sea surface in winter [*Freeland et al., 1998*]. Near its source, NPIW is detected in the upper 1000 m of the water column by its low salinities and high oxygen relative to adjacent water masses [*Yamanaka et al., 1998*]. Interaction with the sea
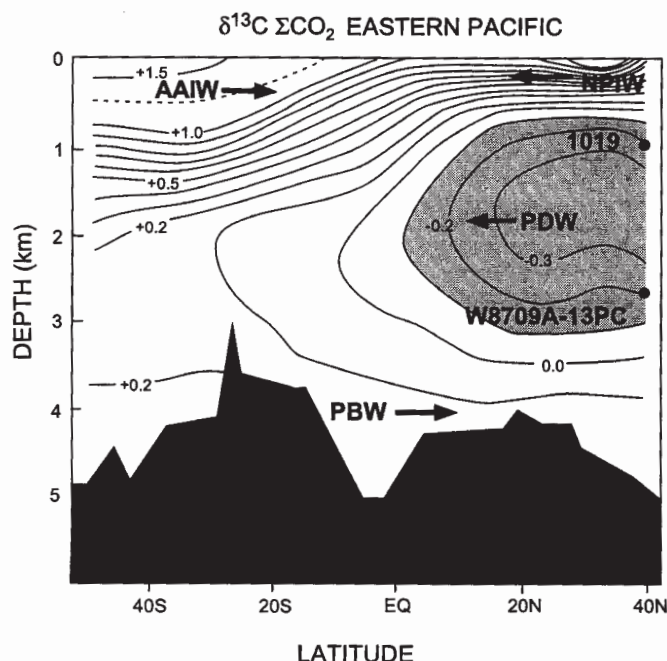
δ¹³C ΣCO₂ EASTERN PACIFIC

Figure 2. Benthic foraminifera in core W8709A-13PC, at 2700 m depth, monitor the mixing zone of low-δ¹³C, high-nutrient Pacific Deep Water (PDW, shaded), and higher-δ¹³C Pacific Bottom Water (PBW). Benthic foraminifera in ODP Site 1019, at 980 m depth, monitor the mixing zone between PDW and relatively high-δ¹³C North Pacific Intermediate Water (NPIW). AAIW is Antarctic Intermediate Water. Contours are δ¹³C of ΣCO₂ in the water column, after Kroopnick [1985].

surface is limited, however, so oxygen levels are low in newly formed NPIW relative to other typical intermediate waters such as Antarctic Intermediate Water (AAIW). This property of relatively low oxygen in NPIW led to original (now discounted) hypotheses that NPIW formed by diapycnal mixing in the absence of substantial interaction with the atmosphere [*Reid*, 1965].

During the Last Glacial Maximum (LGM), increased formation of NPIW in the far northwest Pacific is suggested based on relatively high δ¹³C of benthic foraminifera [*Keigwin*, 1998]. Its penetration appears limited to the upper 2 km of the water column within the Sea of Okhotsk. Enhanced formation of NPIW occurred in spite of apparently greater stratification and stability of the glacial water column in the subpolar North Pacific [*Zahn et al.*, 1991]. A likely mechanism is extreme winter cooling in the northwest Pacific driven by cold, dry winds coming off Asia.

More rapid formation of NPIW at the LGM suggests a hypothesis for the millennial scale, whereby North Pacific cooling, perhaps associated with atmospheric transmission of North Atlantic events such as the Younger Dryas cooling event, also enhanced NPIW formation. Although the timing of events is not firmly constrained, oxic conditions

in the Santa Barbara Basin [*Behl and Kennett*, 1996; *Cannariato et al.*, 1999; *Hendy and Kennett*, 1999] are generally associated with cool events, as predicted by the atmospheric transmission hypothesis. A further test of this hypothesis requires establishing precise dates on changes in upper ocean properties of the North Pacific and the relationship of sea-surface cooling to oxygenation and apparent ventilation in intermediate waters.

3.3. Productivity and the Oxygen Minimum Zone

Another hypothesis to explain variations in anoxia along the California margin is that changes in the biological productivity of the North Pacific modify the intensity of the oxygen minimum zone (OMZ) and the properties of NPIW in the eastern Pacific. Such effects could operate independently of intermediate water formation.

At present, degradation of organic matter raining out of productive North Pacific waters depletes much of the original oxygen in NPIW in the eastern Pacific. Thus, NPIW in the northeast Pacific is detected presently by its density (at shallower depths than in the west) and to some extent by low salinity [*Talley*, 1993]. As a result of high North Pacific productivity and relatively weak ventilation of NPIW, the shallow OMZ of the eastern Pacific margin is strong, approaching anoxia in borderland basins off Southern California and in parts of the Gulf of California.

If millennial-scale intervals of anoxia on the California margin reflect high North Pacific productivity, we would predict seafloor evidence of higher organic rain associated with warmer intervals in the subpolar Pacific. We examine this hypothesis by comparing high-resolution records of organic carbon content in deep-sea sediments, which in the northeast Pacific appears to be driven mainly by changing export productivity [*Lyle et al.*, 1992], with isotopic and faunal estimates of sea surface properties.

3.4. Intermediate and deep waters

Preliminary data on δ¹³C and trace metals in benthic foraminifera from deep northeast Pacific cores suggest millennial-scale variations in mid-depth and deep water properties [*van Geen et al.*, 1997; *Lund and Mix*, 1998]. However, given the limitations of published chronologies it remains uncertain whether the entire deep North Pacific changes in response to upper ocean processes, or whether different water masses record different sources of variability.

Changes in the northward flow rate of Pacific Bottom Water and return southward flow of Pacific Deep Water could modify properties of the deep Pacific from below [*Lund and Mix*, 1998]. Such an effect could be caused by: 1) buoyancy forcing in the Southern Ocean, with a prediction of more bottom water formation near Antarctica during cold intervals [*Rahmstorf*, 1995], 2) variations in westerly winds over the Southern Ocean, which help to maintain geostrophic ventilation of the ocean interior at

mid depths [*Toggweiler and Samuels,* 1993], or 3) by Southern Ocean winds acting as a "flywheel". In this scenario, relatively constant wind-driven demand for total export of deep water to the Antarctic would favor turnover within the deep Pacific when North Atlantic Deep Water sources are reduced [*Lund and Mix,* 1998].

To complicate matters, intermediate water masses formed in either the North or South Pacific could penetrate more deeply into the ocean interior than they do at present. Available $\delta^{13}C$ evidence argues against formation of deep water in the North Pacific during glacial time [*Keigwin,* 1998], but the effects on millennial scales remain uncertain. A modeling study suggests the possibility that Antarctic Intermediate Water could be much stronger in the past, crossing the equator and ventilating the North Pacific at times [*Campin et al.,* 1999], and preliminary data from the Southern Ocean suggest potential changes in such sources [*Ninnemann et al.,* 1997].

Addressing these possibilities, we monitor the deep Pacific at a depth of 2700 m (core W8709A-13PC), in the mixing zone between modern North Pacific deep water and Pacific Bottom Water, and also at a depth of 980 m (Site 1019), in the mixing zone of North Pacific Deep Water and NPIW (Figure 2). If the entire North Pacific were flushed faster or slower, benthic foraminiferal $\delta^{13}C$ records from the two sites would covary. If only intermediate water formed in the North Pacific, then benthic $\delta^{13}C$ would increase at Site 1019 much more than at W8709A-13PC. If the flux rate of bottom waters from the Antarctic increased, the core W8709A-13PC would record the larger changes in deep water properties.

Atmospheric transmission of climatic effects from the North Atlantic to sources of deep water in the North Pacific would imply North Pacific ventilation at times of North Atlantic cooling, although with some lag in the deep Pacific [*Mikolajewicz et al.,* 1997].

Linkages of the deep North Pacific to Southern Ocean forcing would imply different timing of events. For example, buoyancy forcing in the Southern Ocean [*Rahmstorf,* 1995] would predict deep Pacific ventilation events associated with Antarctic cooling, which on millennial time scales has significantly different timing than in the North Atlantic [*Charles et al.,* 1996; *Blunier et al.,* 1998; *Broecker,* 1998].

A mechanism that drives ventilation of the deep interior of the Atlantic and Pacific by varying the strength of Southern Ocean winds [*Toggweiler and Samuels,* 1993] would imply broadly similar oscillations in deep water properties of both oceans. Finally, the "Antarctic Flywheel" effect, in which enhanced deep Pacific ventilation would compensate for reduced sources of North Atlantic Deep Water [*Lund and Mix,* 1998] would suggest opposite changes in the two oceans.

These different scenarios imply very different climate mechanisms for propagating rapid climate changes around the globe. They are not mutually exclusive -- all may operate in concert. At this early stage of research on Pacific climate variability we ask the question whether variations in the proxies for upper ocean circulation, export productivity, and intermediate and deep water properties all change together, or whether differences in signals reveal different linkages in the different systems.

4. METHODS

4.1. Stable Isotopes

All stable isotope data reported here were analyzed at the College of Oceanic and Atmospheric Sciences stable isotope laboratory at Oregon State University, using a Finnigan/MAT 251 mass spectrometer equipped with an Autoprep Systems single acid bath carbonate reaction device.

The benthic foraminifera *Uvigerina sp.* and *Cibicides wuellerstorfi* (3-10 specimens per sample) were hand picked from the >150 μm size fraction. Left-coiling specimens of the planktic foraminifera *Neogloboquadrina pachyderma* (40-50 specimens per sample) were selected from the 150-250 μm fraction (most were near 150 μm). Prior to stable isotopic analysis, foraminifera were cleaned ultrasonically in alcohol and roasted for 1 hr at 400°C under high vacuum to remove organic contaminants. Reactions of carbonates to produce CO_2 gas occurred in ~100% orthophosphoric acid at 90°C.

Precision of isotope analyses of the local OSU carbonate standard was ±0.06°/$_{oo}$ for $\delta^{18}O$ and ±0.03°/$_{oo}$ for $\delta^{13}C$, respectively. Calibration to the widely used Pee Dee Belemnite (PDB) scale was through the NBS-19 and NBS-20 standards provided by the U.S. National Institute of Standards and Technology.

4.2. Radiocarbon

All radiocarbon dates used here are based on accelerator mass spectrometry (AMS) of hand-picked foraminifera. Most of the dates of core W8709A-13PC were published previously [*Gardner et al.,* 1997; *Ortiz et al.,* 1997; *Lund and Mix,* 1998].

New dates presented here for core W8709A-13PC are based on 5-10 mg calcite of monospecific planktonic foraminifera or mixed-species of benthic foraminifera. The foraminifera were ultrasonically cleaned and etched in weak phosphoric acid solution, and then reacted in vaccuo in 100% phosphoric acid. Purified carbon dioxide gas was stored in acid cleaned, pre-roasted, glass tubes and transferred to Lawrence Livermore National Laboratory, where targets were made and analyzed for ^{14}C content (^{13}C corrected).

Radiocarbon dates for samples of ODP Site 1019 were analyzed at the Uppsala AMS facility at University of Uppsala, Sweden, using foraminifera isolated and cleaned at Stockholm University.

Radiocarbon corrections assume a modern reservoir age. At site 1019, inside the coastal upwelling zone, the reservoir age for planktic foraminifera is 800 years [*Robinson and Thompson* 1981; *Southon et al.,* 1990]. The modern reservoir age for planktic foraminifera in core W8709A-13PC, outside the coastal upwelling zone of the northeast Pacific, is 720 years [*Ortiz et al.,* 1997]. For benthic foraminifera, the modern reservoir age is estimated at 1750 years for site 1019, and 2310 years for core W8709A-13PC, based on measured water column radiocarbon contents near 980 m and 2700 m depths in the North Pacific, respectively [*Toggweiler et al.,* 1989].

Radiocarbon dates less than 20,000 reservoir-corrected ^{14}C years old were converted to calendar ages using version 4.1 of the CALIB radiocarbon software [*Stuiver and Reimer,* 1993], which has been updated with recent calibration data sets [*Stuiver et al.,* 1998]. Local reservoir corrections (less 400 years to account for nominal surface ocean radiocarbon ages assumed in CALIB) were entered as constant ΔR values in the CALIB program. An assumed error of ± 200 years was added to ΔR, to account for potential changes in regional reservoir ages. Based on this input, CALIB calculates a time-varying reservoir age and a model-generated history of upper-ocean radiocarbon content driven by changing radiocarbon production terms, as well as a corrected calendar age.

The CALIB software is more appropriately used for oceanic dates based on organisms living in near-surface waters that exchange carbon rapidly with the atmosphere (such as planktonic foraminifera) than it is for deep-sea organisms (such as benthic foraminifera) that may reflect large regional variations in local reservoir ages. Thus, although we used CALIB to calculate calendar ages based on benthic foraminifera, our inferred age models use the results from planktonic foraminifera where possible.

For ages older than 20,000 reservoir-corrected ^{14}C years, we corrected radiocarbon dates to calendar dates using the glacial polynomial algorithm of *Bard* [1998], which is calibrated based on dated corals between about 10,000 and 36,000 ^{14}C years before present.

Calculations of apparent ^{14}C ventilation ages of subsurface waters are made here by subtracting raw ^{14}C dates based on planktic foraminifera from those based on benthic foraminifera in the same samples. The rationale for such calculations is developed by *Broecker et al.* [1984].

4.3. Foraminiferal Species

Samples were hand picked for planktic foraminifera (>150 μm) using CLIMAP taxonomic categories [*Saito et al.,* 1981; *Parker,* 1962], with the exception that we do not recognize the "*pachyderma-dutertrei*" intergrade category of Kipp [1976] in this area. Qualitative estimates of sea-surface temperatures (SST's) are reported as percentages of left-coiling *N. pachyderma* relative to the total number of *N. pachyderma* specimens. An advantage of this method over a total faunal analysis in the northeast Pacific is that it is relatively insensitive to selective dissolution.

Where SST's are less than 5°C, the *N. pachyderma* core-top population is generally comprised of >95% left-coiling specimens. Where sea-surface temperatures are >15°C, the percentages of left-coiling specimens is generally less than 5%. This provides a sensitive faunal indicator of climate off Oregon, where mean annual temperatures range from <10°C (in the coastal upwelling systems) to >15°C (offshore in the California Current). Temperatures during the last glacial maximum are thought to have been 3-4°C cooler than at present in our study area [*Sabin and Pisias,* 1996; *Ortiz et al.,* 1997; *Doose et al.,* 1997].

4.4. Organic Carbon

Accurate measurements of organic carbon content are time consuming, and this limits the ability to generate high-resolution time series needed for assessing millennial-scale changes in export productivity. We get around this limitation by using an optical method, the SCAT system (Split Core Analysis Track), which provides information on sediment composition based on diffuse reflectance spectroscopy of sediment core surfaces [*Mix et al.,* 1992]. The principle is that different sedimentary assemblages have different spectral signatures

The SCAT analyzed 1024 wavelengths ranging from 250-950 nm (Ultraviolet, Visible, and near-Infrared wavelengths). This tool has proven useful in estimating calcium carbonate [*Mix et al.,* 1995; *Harris et al.,* 1997; *Ortiz et al.,* 1999], as well as goethite and hematite contents [*Harris and Mix,* 1999]. Here we use SCAT to estimate organic carbon content.

Calibration of regression equations with low-resolution chemical or mineralogical data yields high-resolution estimates of major changes in sedimentary content. The most reliable estimates off the Oregon and California margin are of organic carbon percentages [*A.C. Mix, unpublished data,* 1999], which can be estimated optically with a standard error of ±0.15%, approaching the analytical precision of some wet chemical methods [*Gardner et al.,* 1997], and sufficient for analysis of relatively large changes observed in Site 1019.

The optical estimates made here, calibrated with 303 measurements made by coulometry aboard D/V JOIDES Resolution in holes 1018A, 1018C, and 1019C [*Lyle et al.,* 1997], provide values of organic carbon content at Site 1019 with an average sample spacing of 150 years during the last deglaciation.

Organic carbon contents in core W8709A-13PC were analyzed by coulometry at Boise State University, with an estimated precision of ±0.05% by weight [*Lyle et al.,* 1999].

5. RESULTS

5.1 Radiocarbon Chronologies

5.1.1. Core W8709A-13PC. AMS radiocarbon dates from core W8709A-13PC are reported in Table 1, and illustrated as calendar corrected ages in Figure 3. Some of these dates were reported earlier [*Lyle et al.*, 1992; *Gardner et al.*, 1997; *Ortiz et al.*, 1997; *Lund and Mix*, 1998]. For clarity we have reproduced those dates in Table 1, correcting some small typographical errors in both age (referring where possible to the original laboratory report) and depth (by re-examining the original sediment core stored at the Oregon State University core laboratory) that have appeared in previous published versions.

There are a few age reversals in core W8709A-13PC. We have chosen to ignore the planktic foraminiferal date at 181 cm, which is younger than the date from 170.5 cm and inconsistent with the benthic date. The planktic date at 196.25 cm depth is older than adjacent dates, and it too is ignored in our inferred age model. Finally, the date on planktic foraminifera at 392.5 cm [*Lyle et al.*, 1992] is younger than adjacent dates and was culled. All three culled samples are included in Table 1, and shown in Figure 3.

Inferred ages in core W8709A-13PC pass through calendar corrected planktic foraminiferal dates in all cases except for the three samples noted above. In these cases, inferred dates pass through both calendar corrected benthic foraminiferal dates, and adjacent planktic foraminiferal dates. Rather than attempt a smooth polynomial fit through the array of dates, we have chosen an objective age model that interpolates linearly between our inferred dates (solid lines in Figure 3). We did not manipulate the age model to improve the correlation of other proxy data between cores or to events elsewhere. We note conservative minimum and maximum age ranges (dashed lines in Figure 3) which are based on the extremes of propagated errors of both benthic and planktic dates.

The new benthic and planktic dates at 170.5 cm and the new benthic date at 181 cm depth in core W8709A-13PC modify the inference of *Lund and Mix* [1998] that a deglacial radiocarbon "plateau" [*Edwards et al.*, 1993; *Hughen et al.*, 1998] was present in this core. Our modification of the age model changes the depth interval of the Younger Dryas interval in core W8709A-13PC (i.e., the depth interval equivalent to calendar ages 11.5-13.0 ka) [*Alley et al.*, 1993] from ~163-191 cm [*Lund and Mix*, 1998] to ~142-165 cm [*this paper*].

5.1.2. Site 1019. AMS radiocarbon data from ODP Site 1019 are reported in Table 2 and illustrated as calendar corrected dates in Figure 4. In most cases the calendar corrected radiocarbon dates from planktic and benthic foraminifera agree well. There are a few exceptions. The planktic foraminiferal date at 5.16 meters composite depth (mcd) in Hole 1019A is anomalously old relative to the benthic date. At 5.82 mcd, the benthic age is anomalously old (Figure 4b). These anomalies may in part reflect changes in reservoir ages through time, due either to changing upwelling intensity (which could change reservoir ages by a few hundred years at most), or to ventilation of thermocline waters with radiocarbon-rich surface waters (which might explain the data at 5.82 mcd), or to ventilation of local bottom waters (at 980 m water depth, this would require lower intermediate water to explain the young benthic date at 5.16 mcd).

Until more data confirm the benthic-planktic age difference patterns we make no attempt to adjust for varying reservoir ages through time (other than that included in the CALIB radiocarbon correction scheme). To avoid age reversals with depth in the core, our inferred age model (solid lines in Figure 4) passes through the calendar corrected benthic foraminiferal date at 5.16 mcd. In all other cases, our inferred age model passes through the calendar corrected planktic foraminiferal dates. As in core W8709A-13PC, we also define minimum and maximum ages (dashed lines in Figure 4) based on propagated errors in both benthic and planktic foraminiferal dates.

We retain all dates from Site 1019 for purposes of calculating benthic-planktic ^{14}C age differences.

5.2. Time Series of Changing Environments

5.2.1. Core W8709A-13PC. Lund and Mix [1998] presented benthic foraminiferal stable isotope data based mostly on the species *C. wuellerstorfi* from core W8709A-13PC. These data are reproduced in Figure 5 along with new data from the genus *Uvigerina* sp., and plotted using the new chronology developed here.

The variations in $\delta^{18}O$ in the two species are very similar but values from *C. wuellerstorfi* are lower by 0.66 ± 0.09 $^o/_{oo}$ (n=185) than those from *Uvigerina* sp. Consistent with previous workers, we added 0.64 to all $\delta^{18}O$ values from *C. wuellerstorfi*.

Changes in $\delta^{13}C$ based on *C. wuellerstorfi* (Figure 5b) suggest that an apparent event of stronger deep-sea ventilation, recorded by $\delta^{13}C$ about 0.2 to 0.3 $^o/_{oo}$ above background values (Figure 5b) occurs from 13.5-12.3 ka, near the beginning or slightly preceding the Younger Dryas interval (shaded following the Greenland Summit, GISP-2, Greenland Ice Sheet Program, ice core $\delta^{18}O$, Figure 5e) [*Grootes et al.*, 1993; *Alley et al.*, 1993].

Variations of $\delta^{13}C$ in *Uvigerina* sp. do not match those of *C. wuellerstorfi* (Figure 5b). *Uvigerina* $\delta^{13}C$ values are on average 0.70 $^o/_{oo}$ (±0.11, n=185) lower than those from *C. wuellerstorfi* in the same samples. In some cases the variations between species are nearly a mirror image. Anomalously low $\delta^{13}C$ values in *Uvigerina* sp. relative to other species are commonly attributed to high organic

Table 1. Radiocarbon data from core W8709A-13PC.

Sample Identifier	Depth (cm)	Sample Type	[14]C Lab	Ref.	[14]C age (ka ± ka)	Res.Cor. age (ka)	Cal. Age (ka ± ka)	Inferred Age (ka)
W8709A-13PC	27.50	Mixed Planktic	CAMS	1	7.00±0.23	6.28	7.22+0.32	7.2
W8709A-13PC	96.25	Mixed Benthic	CAMS	1	11.00±0.12	8.69	9.80±0.43	9.6
W8709A-13PC	98.75	Mixed Benthic	CAMS	1	11.02±0.24	8.71	9.80±0.57	9.7
W8709A-13PC	126.25	Mixed Planktic	CAMS	1	9.96±0.23	9.24	10.31±0.59	10.3
W8709A-13PC	126.25	Mixed Benthic	CAMS	1	11.58±0.17	9.27	10.33±0.56	10.3
W8709A-13PC	128.75	Mixed Benthic	CAMS	1	11.45±0.16	9.14	10.29±0.37	10.5
W8709A-13PC	139.00	Mixed Planktic	CAMS-39369	2	10.72±0.07	10.00	11.33±0.53	11.3
W8709A-13PC	139.00	Mixed Benthic	CAMS-45713	3	12.19±0.06	9.88	11.16±0.39	11.3
W8709A-13PC	154.00	N.pachyderma(L)	CAMS-39370	2	11.20±0.06	10.48	12.33±0.54	12.3
W8709A-13PC	154.00	Mixed Benthic	CAMS-45718	3	12.63±0.06	10.32	11.80±0.61	12.3
W8709A-13PC	170.50	Mixed Planktic	CAMS-45715	3	12.19±0.06	11.47	13.35±0.37	13.3
W8709A-13PC	170.50	Mixed Benthic	CAMS-45714	3	13.08±0.07	10.77	12.71±0.30	13.3
W8709A-13PC	181.00	N.pachyderma(L)	CAMS-39371	2	11.31±0.14	10.59	12.48±0.56	13.6
W8709A-13PC	181.00	Mixed Benthic	CAMS-45719	3	13.88±0.11	11.57	13.45±0.32	13.6
W8709A-13PC	191.50	N.pachyderma(L)	CAMS-44505	3	12.76±0.06	12.04	13.93±0.35	13.9
W8709A-13PC	191.50	Mixed Benthic	CAMS-44506	3	14.33±0.09	12.02	13.95±0.36	13.9
W8709A-13PC	196.25	Mixed Planktic	CAMS	1	13.86±0.10	13.14	15.68±0.32	14.1
W8709A-13PC	196.25	Mixed Benthic	CAMS	1	14.56±0.14	12.25	14.11±0.68	14.1
W8709A-13PC	198.75	Mixed Planktic	CAMS	1	13.00±0.09	12.28	14.13±0.62	14.2
W8709A-13PC	198.75	Mixed Benthic	CAMS	1	14.70±0.25	12.39	14.29±0.73	14.2
W8709A-13PC	212.50	G. bulloides	CAMS-44507	3	13.70±0.07	12.98	15.51±0.67	15.5
W8709A-13PC	212.50	Mixed Benthic	CAMS-44508	3	14.86±0.07	12.55	14.87±0.62	15.5
W8709A-13PC	221.25	Mixed Planktic	CAMS	1	14.05±0.14	13.33	15.90±0.36	15.9
W8709A-13PC	221.25	Mixed Benthic	CAMS	1	15.95±0.18	13.64	16.26±0.38	15.9
W8709A-13PC	223.75	Mixed Planktic	CAMS	1	14.02±0.14	13.30	15.87±0.35	16.0
W8709A-13PC	223.75	Mixed Benthic	CAMS	1	15.77±0.32	13.46	16.05±0.60	16.0
W8709A-13PC	227.5	Mixed Planktic	NZ	4	15.27±0.22	14.55	17.31±0.42	17.4
W8709A-13PC	301.25	Mixed Planktic	CAMS	1	16.71±0.12	15.99	18.96±0.40	19.0
W8709A-13PC	301.25	Mixed Benthic	CAMS	1	18.36±0.20	16.05	19.03±0.44	19.0
W8709A-13PC	303.75	Mixed Planktic	CAMS	1	17.03±0.15	16.31	19.33±0.42	20.0
W8709A-13PC	303.75	Mixed Benthic	CAMS	1	18.63±0.18	16.32	19.34±0.43	20.0
W8709A-13PC	332.5	Mixed Planktic	NZ	4	18.37+0.27	17.65	20.88+0.56	20.9
W8709A-13PC	382.00	G. bulloides	CAMS-39372	2	22.14±0.14	21.42	25.24±0.16	25.1
W8709A-13PC	392.5	Mixed Planktic	NZ	4	19.82±0.64	19.10	22.54+0.83	25.4
W8709A-13PC	401.25	Mixed Planktic	CAMS	1	22.00±0.25	21.28	25.07±0.29	25.7
W8709A-13PC	401.25	Mixed Benthic	CAMS	1	23.56±1.02	21.25	25.04±1.19	25.7
W8709A-13PC	403.75	Mixed Planktic	CAMS	1	21.91±0.24	21.19	24.97±0.28	25.8
W8709A-13PC	403.75	Mixed Benthic	CAMS	1	24.54±0.51	22.23	26.17±0.59	25.8
W8709A-13PC	443.00	G. bulloides	CAMS	2	24.78±0.14	24.06	28.28±0.16	28.3
W8709A-13PC	497.00	G. bulloides	CAMS	2	28.14±0.40	27.42	32.09±0.45	32.1
W8709A-13PC	557.00	G. bulloides	CAMS	2	32.00±0.32	31.28	36.38±0.35	36.4

1) Gardner et al. [1997], 2) Lund and Mix, [1998], 3) This study, 4) Lyle et al. [1992].

carbon rain and a preferred habitat within pore waters [*Zahn et al.*, 1986]. Such an explanation does not fit all the data here, as organic carbon content of the cores does not peak during times of maximum $\delta^{13}C$ offsets between species. If anything, the opposite relationship holds here. Large $\delta^{13}C$ differences between the taxa appear to be associated with lower organic carbon contents (Figure 5d).

The percentage of left-coiling *N. pachyderma* (Figure 5c) is high (essentially 100%, consistent with cold conditions) prior to 15 ka (calendar). Warmer conditions from 13 to 14 ka (50-60% left coiling *N. pachyderma*) are followed by a cold reversal (80-90% left coiling *N. pachyderma*) between 11.5 and 12.5 ka (calendar). A return to warmer conditions occurs at ages < 11.5 ka (calendar).

Given the precision of our age model (inferred ages and minimum-maximum ranges show as horizontal bars in Figure 5a), the oscillation in *N. pachyderma* coiling in core
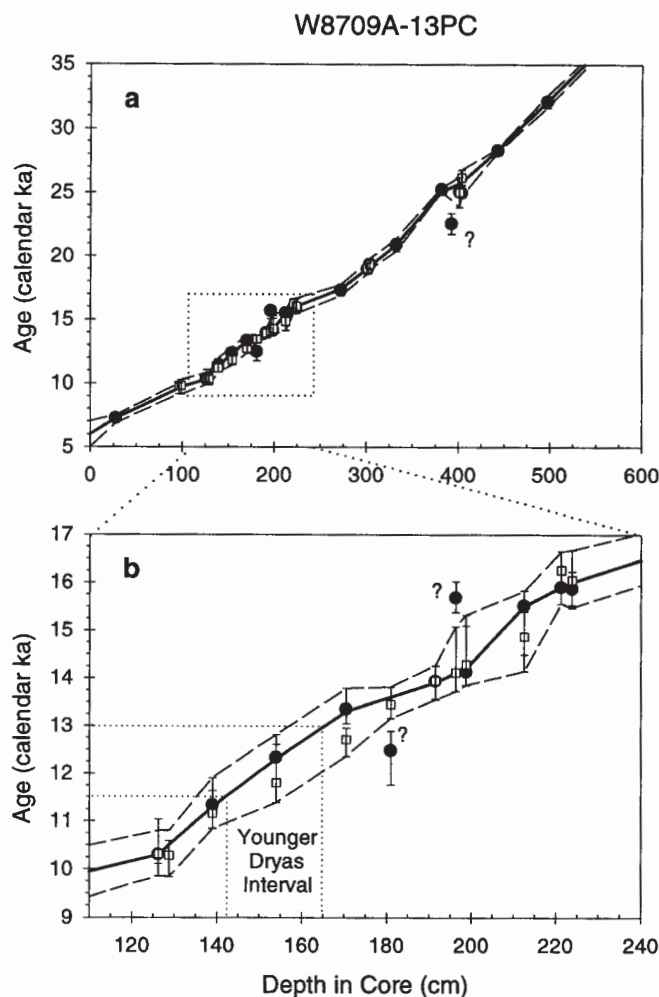
W8709A-13PC

Figure 3. Age model constrained by AMS radiocarbon dates in core W8709A-13PC. All dates are shown as calendar corrected values with ±1σ error bars (see text). Solid circles are dates based on planktonic foraminifera. Open squares are dates based on benthic foraminifera. Question marks indicate suspect dates. The solid line is the inferred age model, and dashed lines mark the upper and lower bounds of propagated errors. a) 5-35 ka (calendar), b) detail of 9-17 ka, illustrating the age control for the Younger-Dryas and Bølling-Allerød intervals.

W8709A-13PC is essentially in phase with the Younger Dryas temperature oscillations in Greenland as recorded by δ¹⁸O in the Greenland Summit (GISP-2) ice core (Figure 5e). Planktic foraminifera are rare in core W8709A-13PC within the Holocene, and the top ~6000 years were not recovered in this core, so with this core we can not assess the extent of variability within the last 10 ka.

5.2.2. Site 1019. Within the coastal upwelling system at a shallower water depth and with high sedimentation rates, Site 1019 reveals additional details of the northeast Pacific variability during the last deglacial period.

The species *C. wuellerstorfi* is less common at Site 1019 than in core W8709A-13PC. The δ¹⁸O of benthic foraminifera *C. wuellerstorfi* and *Uvigerina* sp. (Figure 6a) agree (with an offset between species of 0.68 ± 0.13°/oo, n=38, essentially identical to that in other cores) (Figure 6a).

The δ¹⁸O of planktonic foraminifera *N. pachyderma* (left-coiling) display relatively large oscillations during the last deglaciation, with values about 0.5 to 0.8 °/oo greater (i.e., 2-3°C cooler if entirely attributed to temperature) during the Younger Dryas interval than before or after that event (Figure 6a). This pattern of change is essentially identical to the change in coiling direction of *N. pachyderma*, to more left-coiling specimens during the Younger Dryas event (Figure 6c). Within the limits of the chronology, deglacial warming and cooling at site 1019 are essentially synchronous with similar warming and cooling events recorded in the Greenland Summit (GISP-2) ice core (Figure 6e) [*Grootes et al.*, 1993; *Alley et al.*, 1993].

Site 1019 also records a return to cold conditions (more left-coiling *N. pachyderma* specimens) within the last 8.0 ka. The anomaly appears to be the relatively warm conditions (low percentages of left-coiling) that preceded and followed the Younger Dryas event. In terms of the *N. pachyderma* coiling, mid Holocene conditions appear roughly similar to those of the glacial maximum.

Benthic foraminiferal δ¹³C values at Site 1019, based mostly on *Uvigerina sp.*, are highest relative to background values just prior to and again significantly after the Younger Dryas interval (Figure 6b). Values of δ¹³C in *Uvigerina* sp. are on average 0.58 ± 0.27 °/oo (n=38) lower than those of *C. wuellerstorfi*. There is no apparent decrease in benthic δ¹³C values associated with intervals of high organic carbon content (Figure 6d), so productivity influences on benthic δ¹³C do not appear to be a major problem. To first approximation, δ¹³C data from *Uvigerina* sp. and *C. wuellerstorfi* agree (with an offset), although *C. wuellerstorfi* is often absent, and always rare. Thus, for Site 1019 we use the δ¹³C data from *Uvigerina* sp. as an indicator of bottom water properties. This is not ideal, but is supported by calculations of apparent ventilation ages based on benthic-planktonic differences in radiocarbon dates.

The total range of variation in benthic δ¹³C at Site 1019 (~0.8 °/oo) is large relative to global glacial-interglacial changes δ¹³C of about 0.3 °/oo [*Curry et al.*, 1988]. Average δ¹³C values of *Uvigerina* sp. near the glacial maximum (>18 ka calendar) approach those of the Holocene. Within the Holocene, a ~0.6 °/oo decrease in benthic δ¹³C values occur near 8 ka (calendar), roughly coincident with apparent cooling documented by increases in the percentage of left coiling *N. pachyderma*.

Significant oscillations occur in the δ¹³C of the planktic foraminifera *N. pachyderma* (Figure 6b), but these changes do not appear to be systematically related to warming or

cool events, or organic carbon contents at Site 1019 (Figure 6c,d).

The range or organic carbon concentrations is quite high, from <1 to >4 % (Figure 6d). The organic carbon values are generally low during the cool events recorded by dominance of left coiling *N. pachyderma*. Large increases in organic carbon content occur during warm events recorded locally (Figure 6c) and in the Greenland ice core (Figure 6e). This pattern of higher inferred export production during warm events mimics the glacial-interglacial pattern of paleo-productivity in this region [*Lyle et al.*, 1992; *Ortiz et al.*, 1997].

The similarity of organic carbon percentages at Site 1019 and the temperature oscillations in the Greenland Summit (GISP-2) $\delta^{18}O$ record [*Grootes et al.*, 1993] is striking, especially prior to the Younger Dryas event during the Bølling-Allerød interstade. Although the apparent timing of the organic carbon peaks in Site 1019 appears to lead warm events in Greenland by a few hundred years, given the potential errors in the radiocarbon chronology illustrated by the horizontal bars in Figure 6a, major events in the two regions may be synchronous.

6. DISCUSSION

6.1. Upper ocean changes reflect atmospheric connections.

Both core W8709A-13PC under the offshore California Current and Site 1019 under the coastal upwelling system provide strong support for a cool event (dominance of left-coiling *N. pachyderma*) during deglaciation that is essentially synchronous with the Younger Dryas interval as documented in the Greenland Summit (GISP-2) ice core (Figure 7). This finding supports the concept of rapid atmospheric transmission of millennial-scale warming and cooling cycles between the Atlantic and the Pacific.

Based on the range of planktonic foraminiferal $\delta^{18}O$ values before, during, and after the Younger Dryas event (0.5-0.7 $^o/_{oo}$, Figure 6), we estimate the range of upper-ocean temperature changes at Site 1019 to be 2-3°C (assuming no other changes). This extent of change is smaller than surface water changes recorded in the Santa Barbara Basin, where $\delta^{18}O$ data from planktic foraminifera suggest rapid temperature oscillations of 4-8°C [*Hendy and Kennett*, 1999]. In both areas, observed changes in temperature are higher than those predicted by a coupled ocean-atmosphere model, ~1°C near the eastern boundary of the North Pacific [*Mikolajewicz et al.*, 1997].

Our finding of significant oscillations in near-surface conditions that are essentially synchronous presents an opportunity to use this oscillation as a stratigraphic marker. By comparing variations of other properties in the same samples in these northeast Pacific cores, we can place a range of processes, including variations in deep water properties, into a well constrained stratigraphy to examine dynamics of the North Pacific system during this interval.

6.2. Mid-Holocene cooling: An abrupt response to orbital forcing?

Site 1019 reveals that, for the northeast Pacific at least, the warm events recorded by the coiling of the planktonic foraminifera *N. pachyderma*, which precede and follow the Younger Dryas interval, are anomalous relative to typical late Holocene conditions. The coastal upwelling system of the Northern California Current appears to have returned toward its ice-age state about 8,000 years ago, following brief warm episodes during the deglaciation (Figure 7). This sense of change is supported by an increase in $\delta^{18}O$ of *N. pachyderma* at the same time; however a return to lower $\delta^{18}O$ values near 6,000 years ago, with little change in the *N. pachyderma* coiling ratio, implies significant reduction of upper ocean salinities in the region without major temperature change (Figure 6).

This result based on *N. pachyderma* coiling supports the earlier, lower-resolution, finding of mid-Holocene cooling in the Alaska Gyre based on radiolarian faunas [*Sabin and Pisias*, 1996]. To the south, *Pisias* [1979] inferred similar mid-Holocene cooling in the Santa Barbara Basin along with a change in short-term variability. Consistent with the changes we find to the north, the apparent cooling off Southern California was associated with an increase in the percentage of the fauna that resides in the eastern boundary current.

Mid-Holocene cooling of the northeast Pacific also matches reductions in land temperature inferred from pollen in coastal Washington [*Heusser et al.*, 1980] and British Columbia [*Mathewes and Heusser*, 1981], and from alpine glacier advances near 5.7 and 3.9 ka [^{14}C ages; *Burke and Birkeland*, 1983; *Davis*, 1988]. Analogous mid-Holocene cooling, possibly synchronous with the events of the North Pacific, also occurred in the Arctic and North Atlantic regions [*Kerwin et al.*, 1999]. Thus, the mid-Holocene cooling of the northeast Pacific documented here may be part of a widespread phenomenon in the high-latitude regions of the Northern Hemisphere.

The cause of such mid-Holocene cooling is unknown. One possibility is that gradual reduction in summer (and increase in winter) insolation through the Holocene, associated with well-known changes in Earth's orbit, may have resulted in expansion of polar waters in the Northern Hemisphere. Mechanisms related to orbital insolation change may include gradual reduction of direct summer heating of the subpolar North Pacific, which would cool the ocean directly, and weaker winter cooling, which could suppress formation of NPIW and the associated northward advection of upper ocean heat.

The relatively rapid change observed near 8000 years ago implies a threshold response to the gradual change in insolation. An abrupt shift might be expected from a mechanism that includes intermediate water formation during the early Holocene warm intervals. Enhanced intermediate water formation at these times would help to

Table 2. Radiocarbon data from ODP Site 1019 (all dates new to this paper).

Sample Identifier	DIC[1] (m)	MCD[2] (m)	Sample Type	[14]C Lab Ref. No.	[14]C age (ka ± ka)	Res Cor Age (ka)	Cal. Age (ka ± ka)	Inferred Age (ka)
1019A01H1 40-46 cm	0.43	2.84	bark	UA11171	6.03±0.15	6.03	6.82±0.24	6.8
1019A01H2 22-28 cm	1.75	4.17	Mixed Planktic	UA12954	9.95±0.11	9.15	10.29±0.37	10.1
1019A01H2 22-28 cm	1.75	4.17	Mixed Benthic	UA12955	10.81±0.12	9.06	10.27±0.16	10.1
1019A01H2 97-103 cm	2.51	4.92	Mixed Planktic	UA11246	10.21±0.12	9.41	10.45±0.41	10.6
1019A01H2 97-103 cm	2.51	4.92	Mixed Benthic	UA11662	11.13±0.08	9.38	10.48±0.41	10.6
1019A01H2 122-128 cm	2.75	5.16	Mixed Planktic	UA12956	11.41± 0.17	10.61	12.47±0.57	11.2
1019A01H2 122-128 cm	2.75	5.16	Mixed Benthic	UA12957	11.54±0.09	9.79	11.12±0.39	11.2
1019A01H3 38-44 cm	3.40	5.81	Mixed Planktic	UA12958	11.58±0.14	10.78	12.70±0.32	12.7
1019A01H3 38-44 cm	3.40	5.81	Mixed Benthic	UA12959	13.29±0.22	11.54	13.43±0.38	12.7
1019A01H3 78-84 cm	3.80	6.21	Mixed Planktic	UA12960	11.95±0.11	11.15	13.02±0.15	13.0
1019A01H3 78-84 cm	3.80	6.21	Mixed Benthic	UA12961	12.83±0.09	11.08	12.99±0.24	13.0
1019A01H4 24-30 cm	4.76	7.11	Mixed Planktic	UA11867	13.35±0.12	12.55	14.87±0.63	14.8
1019A01H4 24-30 cm	4.76	7.11	Mixed Benthic	UA11866	14.26±0.14	12.51	14.34±0.63	14.8
1019A01H4 128-134 cm	5.80	8.21	Mixed Planktic	UA12962	15.08±0.12	14.28	17.00±0.36	17.0
1019A01H4 128-134 cm	5.80	8.21	Mixed Benthic	UA12963	16.21±0.19	14.46	17.20±0.40	17.0
1019A01H5 110-116 cm	7.13	9.54	Mixed Planktic	UA11531	16.04±0.14	15.24	18.10±0.39	18.1
1019A01H5 110-116 cm	7.13	9.54	Mixed Benthic	UA11663	17.48±0.28	15.73	18.66±0.49	18.1
1019A01H6 60-66 cm	8.14	10.55	Mixed Planktic	UA12964	18.55±0.21	17.75	20.98±0.47	21.0
1019A01H6 60-66 cm	8.14	10.55	Mixed Benthic	UA12965	19.08±0.19	17.33	20.51±0.45	21.0
1019A01H7 71-77 cm	9.74	12.15	Mixed Planktic	UA11865	21.24±0.28	20.44	23.95±0.54	24.0
1019A01H7 71-77 cm	9.74	12.15	Mixed Benthic	UA11864	23.86±0.86	22.11	25.85±1.18	24.0

[1]DIC is depth in core. [2]MCD is meters composite depth [Lyle et al., 1997].

amplify warming and sustain circulation by drawing warm and salty water northward from the subtropics. This concept is discussed in more detail in section 6.4 below.

Model experiments indicate that climates in North America, including extent of snow cover and potential for glaciation, are sensitive to sea surface temperatures in the North Pacific [Peteet et al., 1997]. This is particularly interesting in light of inferences based on the phase of climate cycles in various regions, that the earliest cooling events in the global response to orbital forcing must be in the Northern Hemisphere [Imbrie et al., 1989]. Whether the high latitude North Pacific plays a role in triggering these ice age cycles awaits the availability of longer time series of upper ocean temperatures in this region, and more detailed models of the downstream impacts of North Pacific cooling on climates in North America and elsewhere.

6.3. Variability in the North Pacific oxygen minimum zone: Productivity or intermediate water formation?

Two hypotheses are available to explain available data on the well known millennial-scale oscillations in oxygen minimum zone of the northeast Pacific [Kennett and Ingram, 1995; Behl and Kennett, 1996; Cannariato et al., 1999]. First, enhanced formation of intermediate or thermocline waters in the North Pacific during cold events could change oxygenation in the Santa Barbara Basin and California Margin. Second, increased export productivity during warm intervals might have increased consumption of oxygen in the thermocline of the North Pacific, resulting in anoxia on the California margin.

This second hypothesis appears to be viable. Organic carbon burial at site 1019 is highest during warm events (essentially coincident with the Bølling-Allerød interstade and early Holocene warmth; Figure 7), which are also times of consistent anoxia in the OMZ [Behl and Kennett, 1996]. These events include the presence of diatom mats at Site 1019 [Lyle et al., 1997], which are associated with high-export ecosystems, and also with increased abundance of coastal upwelling diatom assemblages during early Holocene warmth [Sancetta et al., 1992]

Of course, this inference begs a question of what drives the change in export productivity. At present, productivity of the North Pacific ecosystem is not limited by the major nutrients phosphate and nitrate. One possibility is iron limitation. A primary source of iron to the North Pacific is resuspension of sediments deposited on continental shelves and offshore advection in strong coastal upwelling systems [Johnson et al., 1999]. In the northeast Pacific, such strong coastal upwelling occurs at present during summer [Huyer, 1983], and on longer time scales is associated with warm intervals. During cold climatic intervals, coastal upwelling was reduced due to suppression of northerly summer winds [Lyle et al., 1992; Ortiz et al., 1997]. A likely consequence of enhanced iron input associated with coastal upwelling is to favor productive ecosystems that include large diatoms which are more efficiently exported from the sea surface
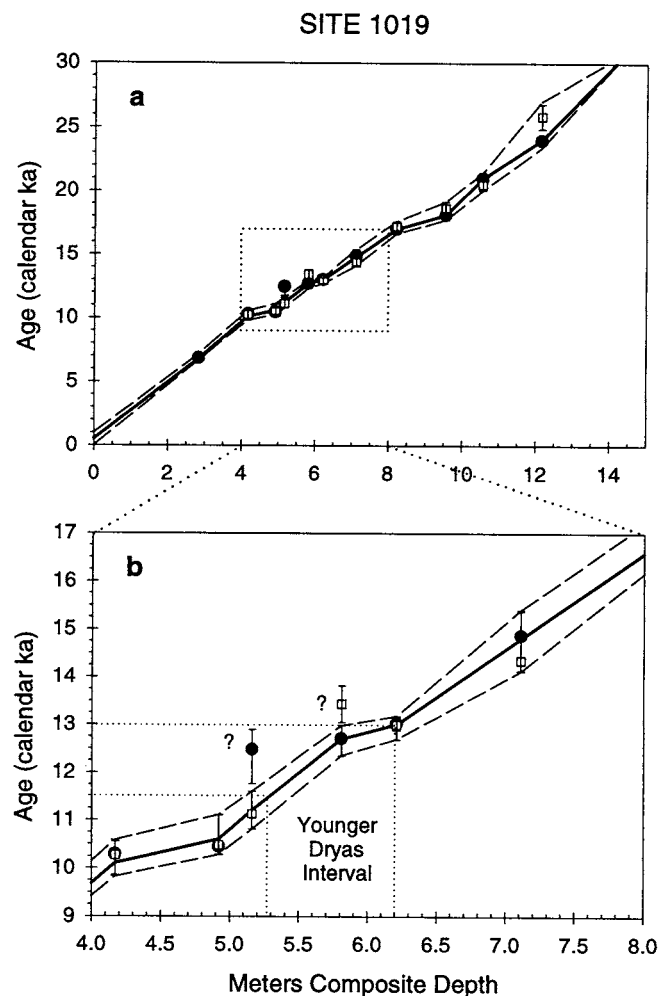
Figure 4. Age model constrained by AMS radiocarbon dates in ODP Site 1019. All dates are shown as calendar corrected values with ±1σ error bars (see text). Solid circles are dates based on planktonic foraminifera. Open squares are dates based on benthic foraminifera. Question marks indicate suspect dates. The solid line is the inferred age model, and dashed lines mark the upper and lower bounds of propagated errors. a) 0-3 ka (calendar), b) detail of 9-17 ka, illustrating the age control for the Younger-Dryas and Bølling-Allerød intervals.

[*Hood et al.*, 1990; *Takeda*, 1998]. The net effect would be enhanced export of organic matter and depletion of oxygen in subsurface waters during intervals of warmth in the northeast Pacific. Such a linkage may help to explain the variations in anoxia in Santa Barbara Basin during the deglacial interval [*Behl and Kennett*, 1996; *Cannariato et al.*, 1999].

We can not exclude the possibility of greater ventilation of thermocline waters in the range of a few hundred meters water depth during cold intervals. Arguments in favor of such ventilation include an apparent reduction in the ^{14}C age difference between benthic and planktic foraminifera

within Santa Barbara Basin during the Younger Dryas event [*Kennett and Ingram*, 1995]. During deglacial times, the sill depth of the Santa Barbara Basin was about 350-400 m. The modern density at these depths off southern California approaches that of the winter mixed layer in the far North Pacific [*Van Scoy et al.*, 1991]. Thus, it is likely that the Santa Barbara Basin and the oxygen minimum zone off California would have been more sensitive to deep winter mixing and formation of subpolar mode waters in the past. Below we suggest, however, that increases in water ventilation events during the Younger Dryas cooling did not necessarily include NPIW.

6.4. Ventilating intermediate waters: A northern source?

Increases in benthic foraminifera δ^{13}C and decreases in the radiocarbon age differences between benthic and planktic foraminifera are potential indicators of sub-surface ventilation in the North Pacific. Both tracers are compromised to some extent by gas exchange processes [*Broecker et al.*, 1984; *Broecker and Maier-Reimer*, 1992; *Campin et al.*, 1999]. Greater exchange with the atmosphere at high latitudes would increase the δ^{13}C value and decrease the preformed radiocarbon age of a cold, newly formed subsurface water mass, independent of changes in the rate of watermass formation. Thus, ventilation of the deep sea could be accomplished either by greater rates of watermass formation, or by increases in gas exchange.

At ~980m water depth, Site 1019 presently samples the mixing zone between NPIW and Pacific Deep Water (Figure 2). At this site, relatively high benthic foraminiferal δ^{13}C is closely associated with upper-ocean warmth in the Bølling-Allerød interstade, and in the early Holocene (Figure 8). Even though this record is based on the genus *Uvigerina* sp., which is sometimes compromised by productivity overprints on the δ^{13}C record, we tentatively accept it as an approximate record of watermass variability here. We have shown that the δ^{13}C record does not appear to be an artifact of productivity, because it changes in the opposite sense that would be expected based on organic carbon contents of the sediment.

An inference of greater ventilation of intermediate water during the early Holocene and deglacial warm intervals is supported by data on the radiocarbon age differences between benthic and planktic foraminifera. At site 1019, this difference has greater than modern values (implying lower ventilation) during the Younger Dryas cold interval, and less than modern values (implying more rapid ventilation) during the early Holocene warm interval (Figure 8a).

The relatively close linkage between benthic δ^{13}C at Site 1019 and the deglacial oscillations in the Greenland ice core (Figure 8) argues for atmospheric transmission of signals and a northern-hemisphere source of the watermass, but not in the sense first hypothesized. On the millennial
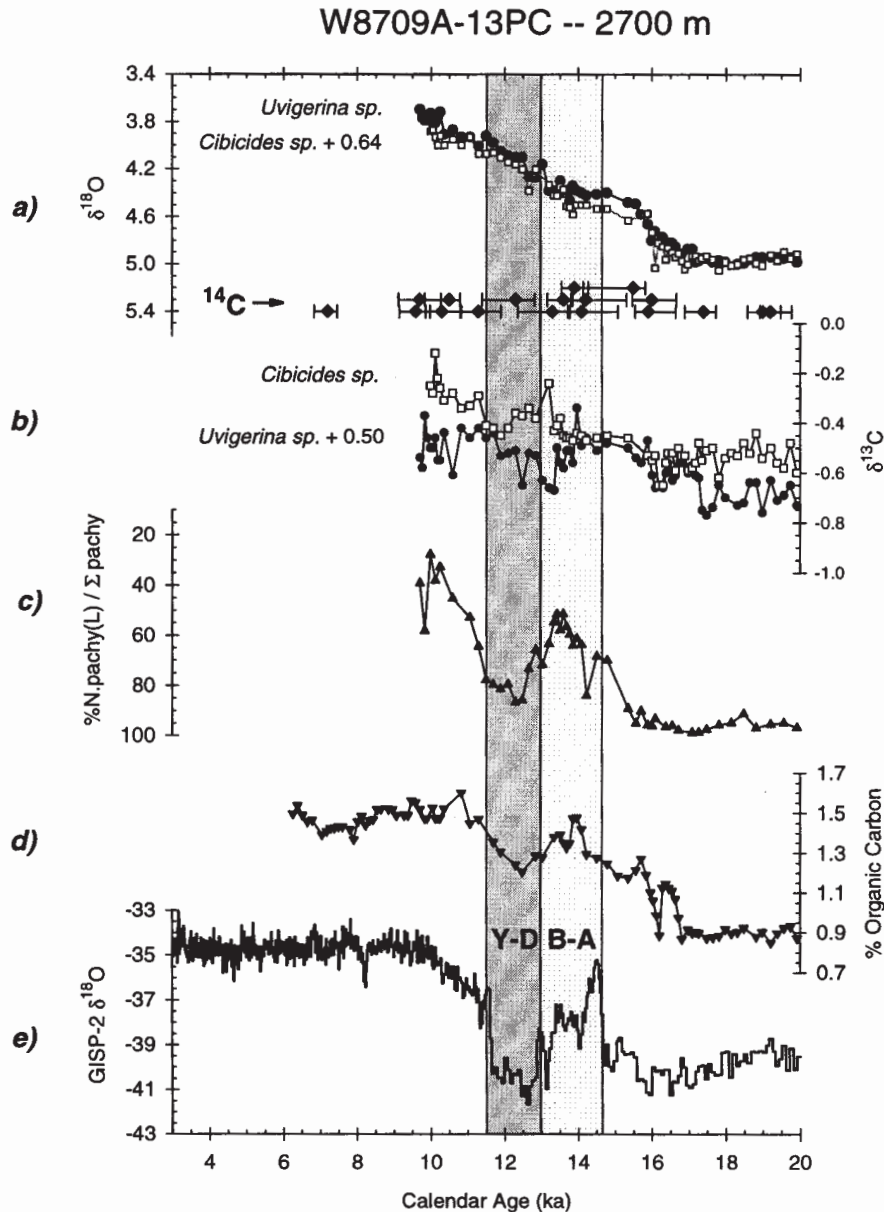
W8709A-13PC -- 2700 m

Figure 5. Time series in core W8709A-13PC, based on linear interpolation of the inferred age model in Figure 3. Shaded bars indicate the Younger Dryas (Y-D) and Bølling Allerød (B-A) intervals. a) Benthic foraminiferal $\delta^{18}O$. Open squares are *C. wuellerstorfi* + 0.64. Filled circles are *Uvigerina sp.* Filled diamonds are inferred ages. Horizontal bars indicate the range of the minimum and maximum age models at each inferred age datum. b) Benthic foraminiferal $\delta^{13}C$. Open squares are *C. wuellerstorfi*. Solid circles are *Uvigerina sp.* + 0.50. c) The percentage of left-coiling *N. pachyderma* relative to total *N. pachyderma*. d) Weight % organic carbon. e) Greenland Summit (GISP-2) ice core $\delta^{18}O$ (‰ relative to SMOW, data from Grootes et al., [1993], timescale from Alley et al., [1993]) for reference.

scale, our data suggest greater ventilation of mid-depth waters during warm, not cold events. To the extent that the $\delta^{13}C$ and ^{14}C data from Site 1019 record variations in NPIW formation rates, they would suggest that NPIW formation is not responsible for the apparent variations in the OMZ on the California margin.

The possibility of significant intermediate water coming from a North Pacific source during the early Holocene and deglacial warm intervals suggests that higher salinity, rather than cooling, may have provided the density required for formation. This is different from, but not necessarily in conflict with, the glacial maximum situation in which
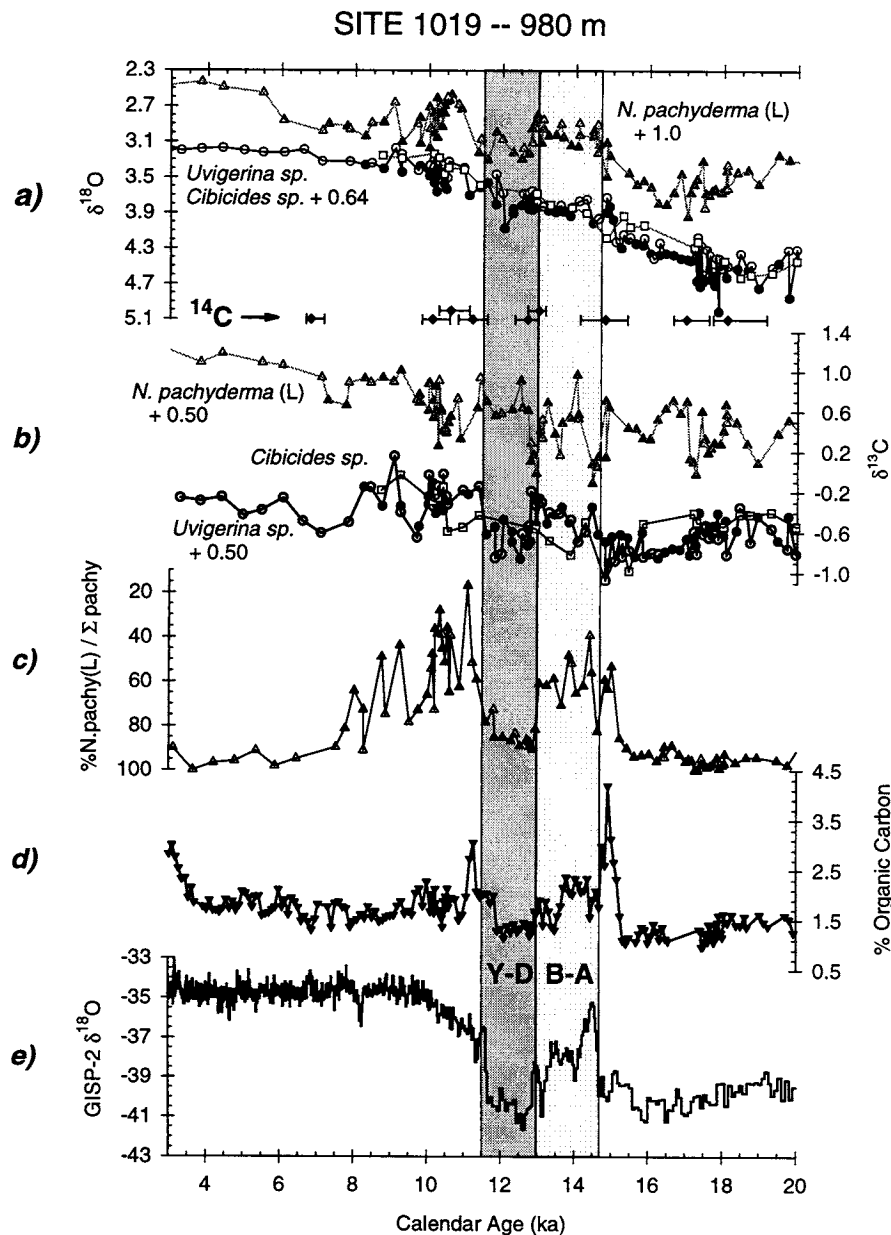
Figure 6. Time series in ODP Site 1019, based on linear interpolation of the inferred age model in Figure 4. Shaded bars indicate the Younger Dryas (Y-D) and Bølling Allerød (B-A) intervals. a) $\delta^{18}O$ ($^o/_{oo}$ relative to PDB). Open squares are *C. wuellerstorfi* + 0.64, from hole 1019c. Filled circles are *Uvigerina* sp. from hole 1019c. Open circles are *Uvigerina* sp. from hole 1019a. Filled triangles are left-coiling *N. pachyderma* + 1.0, from hole 1019a. Open triangles are left-coiling *N. pachyderma* + 1.0, from hole 1019a. Filled diamonds are inferred ages, and horizontal bars indicate the range of the minimum and maximum age models at each inferred age datum. b) $\delta^{13}C$. ($^o/_{oo}$ relative to PDB). Open squares are *C. wuellerstorfi*, from hole 1019c. Filled circles are *Uvigerina* sp. + 0.50 from hole 1019c. Open circles are *Uvigerina* sp. + 0.50 from hole 1019a. Filled triangles are left-coiling *N. pachyderma* + 0.50, from hole 1019a. Open triangles are left-coiling *N. pachyderma* + 0.50, from hole 1019a. c) The percentage of left-coiling *N. pachyderma* relative to total *N. pachyderma*. Solid triangles are from hole 1019a. Open triangles are from hole 1019c. d) Weight % organic carbon in hole 1019c. e) Greenland Summit (GISP-2) ice core $\delta^{18}O$ ($^o/_{oo}$ relative to SMOW, data from Grootes et al., [1993], timescale from Alley et al., [1993]).
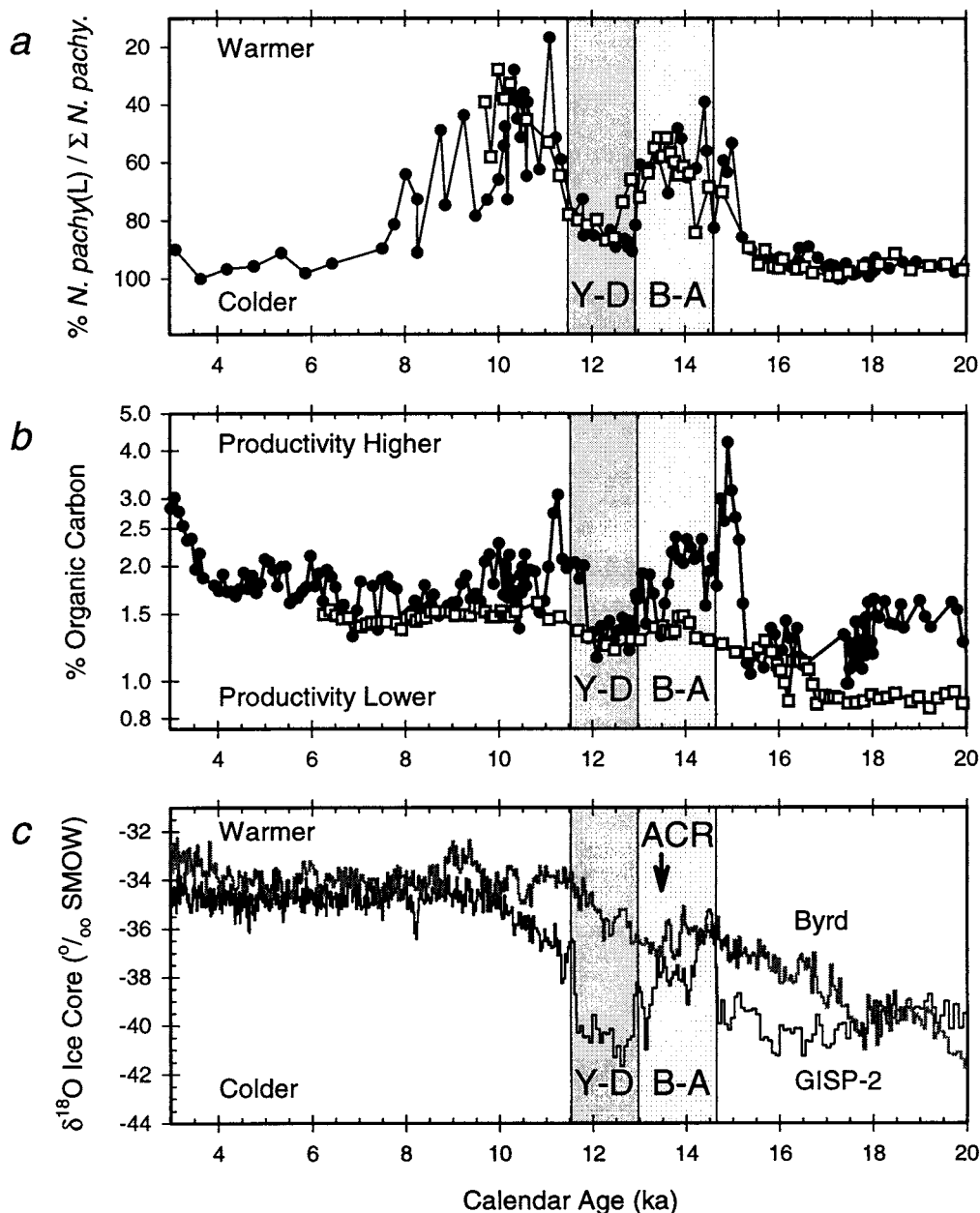
Figure 7. Upper ocean proxies in core W8709A-13PC and ODP Site 1019. a) The percentage of left-coiling *N. pachyderma* relative to total *N. pachyderma*. Filled circles are from Site 1019. Open circles are from core W8709A-13PC. Lower values (up on the graph) indicate warmer conditions. Note approximate synchrony between the two sites, the good match of cooling with the Younger Dryas interval, and apparent mid-Holocene cooling near 8 ka (calendar). b) Percentages of organic carbon in hole 1019C (filled circles) and core W8709A-13PC (open circles) plotted on a log scale. Higher values suggest higher export productivity. Note that high values correspond to warm intervals in (a). c) For comparison, Greenland Summit (GISP-2) ice core $\delta^{18}O$ ($^o/_{oo}$ relative to SMOW, black line, data from Grootes et al., [1993], timescale from Alley et al., [1993]) defines the ages of the Younger Dryas (Y-D) and Bølling-Allerød (B-A) intervals. Byrd Ice Core $\delta^{18}O$ ($^o/_{oo}$ relative to SMOW, gray line, data from Johnsen et al., [1972], timescale from Bender et al., [1999]) define the timing of the Antarctic Cold Reversal (ACR). The upper ocean proxies from the North Pacific are better correlated to $\delta^{18}O$ data from Greenland than to $\delta^{18}O$ data from Antarctica.

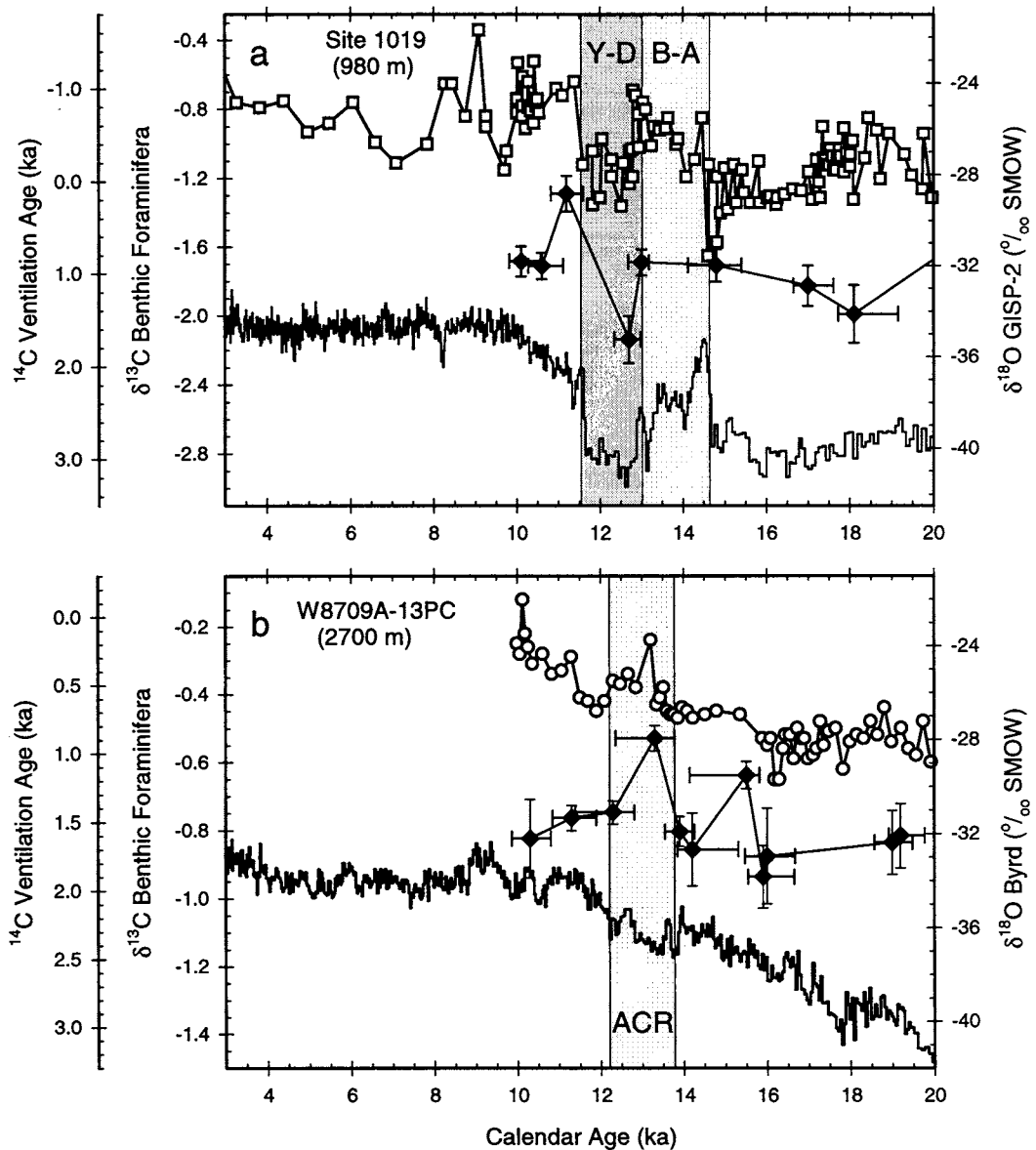**Figure 8.** Deep ocean proxies from the northeast Pacific. a) In ODP Site 1019, benthic foraminiferal $\delta^{13}C$ (based on Uvigerina sp., open squares) are lower during the Younger Dryas (Y-D) interval and higher during the Bølling-Allerød and early Holocene intervals, suggesting greater ventilation at 980m depth during warm events in the North Pacific. This inferences is supported by estimates of ^{14}C ventilation age, the difference between benthic and planktonic ^{14}C dates (filled diamonds with error bars). Lower values (up on graph) indicate faster replacement of lower intermediate waters, or a greater $^{14}C/^{12}C$ of the water mass when it left the sea surface. Greenland Summit (GISP-2) ice core $\delta^{18}O$ ($^o/_{oo}$ relative to SMOW, black line, data from Grootes et al., [1993], timescale from Alley et al., [1993]) defines the ages of the Younger Dryas (Y-D) and Bølling-Allerød (B-A) intervals. b) In core W8709A-13PC benthic foraminiferal $\delta^{13}C$ (based on C. wuellerstorfi., open circles) are high relative to background values during the Antarctic Cold Reversal (ACR, 12.3-13.8 ka calendar) and near 10 ka (calendar), suggesting that greater ventilation at 2700 m depth is associated with cold events in the Southern Ocean. This inference based on $\delta^{13}C$ is supported by estimates of ^{14}C ventilation age, the difference between benthic and planktonic ^{14}C dates (filled diamonds with error bars). Lower values (up on graph) indicate faster replacement of deep or bottom waters, or a greater $^{14}C/^{12}C$ of the water mass when it left the sea surface. $\delta^{18}O$ in the Byrd Ice Core ($^o/_{oo}$ relative to SMOW, black line, data from Johnsen et al., [1972], timescale from Bender et al., [1999]) define the timing of the ACR.

stronger sources of intermediate water in the Sea of Okhotsk were associated with ice-age cooling [*Keigwin, 1998*].

Active formation of NPIW during millennial-scale warm events may provide a mechanism to explain the range of temperature changes observed in the California Current region [*Hendy and Kennett, 1999; this paper*], which is higher than that predicted by a coupled atmosphere-ocean model simulation [*Mikolajewicz et al., 1997*]. Regional warmth in the North Pacific would increase evaporation rates and sea-surface salinities, possibly leading to intermediate water formation that would help to advect more oceanic heat (and salt) northward from the subtropics. This link essentially reverses the causal chain of *Warren* [1983] and provides a plausible feedback mechanism to amplify upper ocean temperature changes in the North Pacific. It also implies that the North Pacific may be susceptible to rapid shifts in its mode of circulation between two potentially stable states.

6.5. Ventilating deep waters: A southern source?

Deeper in the water column (~2700 m), benthic foraminiferal $\delta^{13}C$ from the species *C. wuellerstorfi* and benthic-planktic ^{14}C age differences suggest a somewhat different history of ventilation (Figure 8b). Here, in the mixing zone between northward flowing Pacific Bottom Water and southward flowing Pacific Deep Water, high apparent ventilation (inferred from high $\delta^{13}C$ and a low benthic-planktic ^{14}C age difference) occurs near 13 ka (calendar).

This ventilation event appears to be poorly correlated with the Younger Dryas oscillation of the Northern Hemisphere, but is essentially in phase with the Antarctic Cold Reversal (ACR) as documented by relatively low $\delta^{18}O$ in the Byrd Ice Core ($\delta^{18}O$ from *Johnsen et al.* [1972], timescale from *Bender et al.* [1999]). Additional high $\delta^{13}C$ values, suggesting greater ventilation of the deep Pacific, occur near 10 ka (calendar), coincident with another cooling event in Antarctica.

Thus, the pattern of isotopic variation in the deep North Pacific suggests the possibility of greater ventilation coming from the Southern Hemisphere, transmitted northward via bottom waters. This finding is based on limited data and remains somewhat uncertain based on the chronologic constraints. The inference is strengthened, however, by the stratigraphic relationship of benthic foraminiferal $\delta^{13}C$ and apparent Younger-Dryas cooling of surface waters recorded in the same core samples. If our inference is correct, it implies that the time signature of millennial-scale oscillations in the Northern and Southern Hemisphere, now referred to as a bi-polar seesaw [*Broecker, 1998; Charles et al., 1996*], will be detected elsewhere at different depths within the Pacific.

6.6. Deep-sea temperatures and Antarctic warming.

Benthic foraminiferal $\delta^{18}O$ values in Site 1019 (all corrected to equivalent *Uvigerina* sp. values) vary from ~3.1 $^o/_{oo}$ to ~4.8 $^o/_{oo}$, a range of more than 1.7 $^o/_{oo}$ (Figure 9). Although samples from W8709A-13PC do not reach the late Holocene, glacial values reach 5.0 $^o/_{oo}$. Late Holocene values in nearby cores are about 3.3 $^o/_{oo}$. This range of $\delta^{18}O$ of more than 1.6 $^o/_{oo}$ is important, because if recent estimates are correct that the amplitude of the ice-volume driven change in mean oceanic $\delta^{18}O$ is about 1.0 $^o/_{oo}$ [*Schrag et al., 1996*] then the deep North Pacific (at 980m) may have cooled at the last glacial maximum by about 3°C. At present, the temperatures of water in contact with the sea floor at Site 1019 and at W8709A-13PC are 3.6°C and 1.6°C, respectively, so ice-age water temperatures here would have been <1°C at 980m depth and <-1°C at 2700 m depth.

The time series of benthic foraminiferal $\delta^{18}O$ are compared to sea level estimates from Barbados corals [*Fairbanks, 1989*], and to $\delta^{18}O$ data from the Byrd ice core in Antarctica [*Johnsen et al., 1972; age model of Bender et al., 1999*] in Figure 9. This plot overlays sea level on oceanic $\delta^{18}O$ with the scaling implied by Barbados coral data of 0.11$^o/_{oo}$ per 10 m [*Fairbanks and Matthews, 1978*]. If the *Schrag et al.* [1996] scaling of sea level relative to $\delta^{18}O$ was used, deviations between these records would be even larger.

Through much of the transition, benthic $\delta^{18}O$ and sea level are essentially coincident (within the limits of the chronology). A major deviation occurs between sea level and benthic $\delta^{18}O$ in both cores prior to ~15.5 ka (calendar). Although sea level data are sparse in this interval, it is unlikely that values are much lower than the three dated points between 18 and 19 ka (calendar) [*Fairbanks, 1989*]. Recent summaries indicate very little melting of Northern Hemisphere ice sheets in this interval, and suggest that much of the melting associated with the ~14 ka (calendar) sea level rise occurred in Antarctica [*Clark et al., 1996*]. A likely conclusion based on the deviation between benthic $\delta^{18}O$ and sea level is that significant warming of the deep sea occurred prior to ~15.5 ka (calendar) without major change in sea level (and thus without major melting of ice sheets).

Comparison of the benthic foraminiferal $\delta^{18}O$ records to the Byrd ice core $\delta^{18}O$ suggests that early warming of the deep Pacific may be coincident with early warming in Antarctica (Figure 9). Similar early warming in surface waters have been observed in the subantarctic region [*Charles et al., 1996; Broecker, 1998*]. If true, this implies that sea surface conditions near Antarctica are important in setting the heat budget of the deep sea, at least in regions where Antarctic Bottom Water is an important contributor to abyssal water masses.
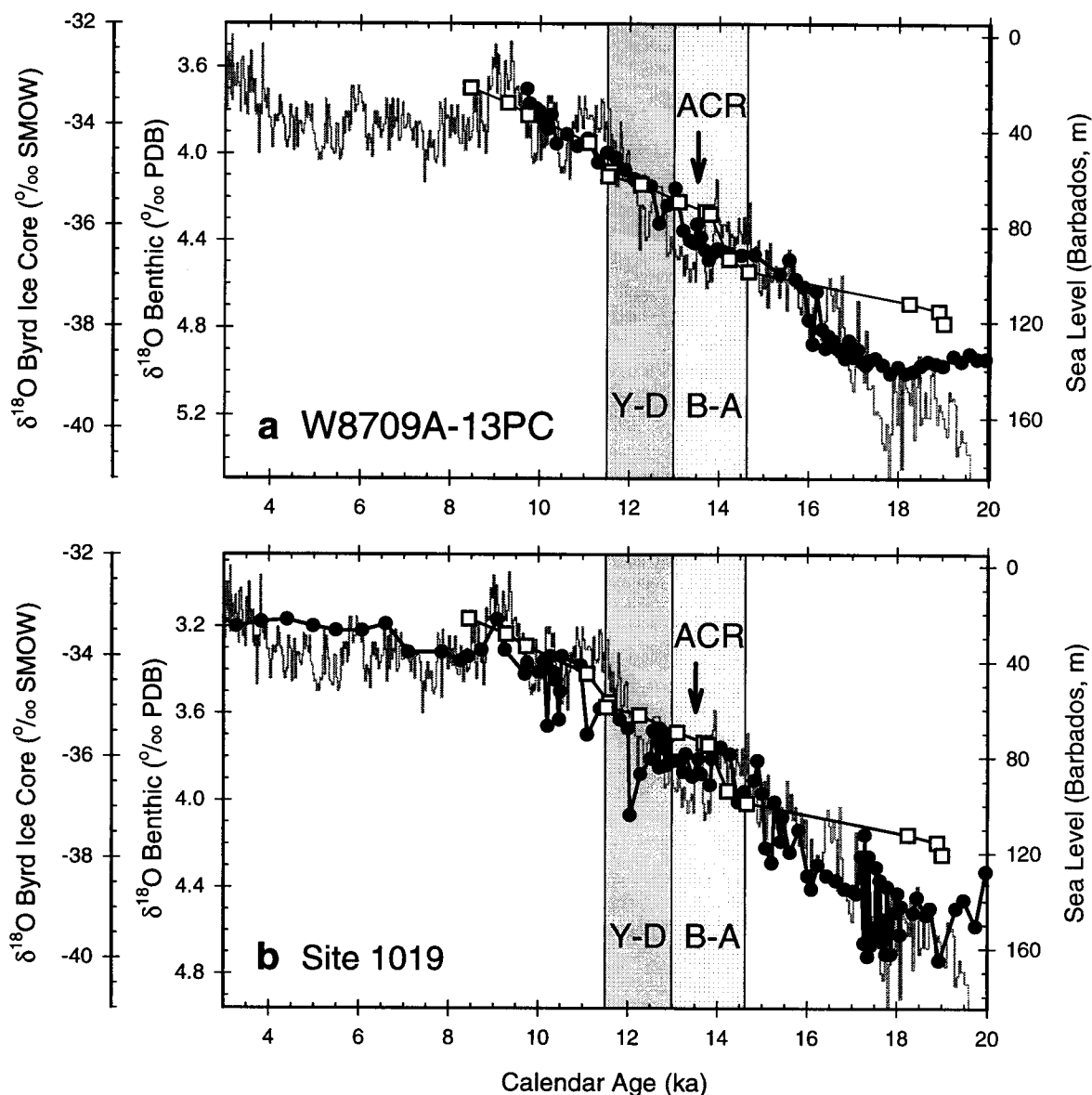
Figure 9. Benthic foraminifera $\delta^{18}O$ data ($^o/_{oo}$ PDB, filled circles), including data from *C. wuellerstorfi (+0.64)* and *Uvigerina* sp., are compared to sea level data (open squares) from Barbados [*Fairbanks,* 1989], and $\delta^{18}O$ in the Byrd Ice Core ($\delta^{18}O$ SMOW, black line, data from Johnsen et al., [1972], timescale from Bender et al., [1999]). Bars note the timing of the Younger Dryas (Y-D) and Bølling-Allerød (B-A) intervals [*Alley et al.,* 1993]. a) Core W8709A-13PC (2700 m water depth), b) ODP Site 1019 (980 m water depth).

7. CONCLUSIONS

Planktonic foraminiferal species abundances, benthic and planktonic foraminiferal stable isotopes, radiocarbon, and organic carbon content of deep-sea cores off Oregon and California reveal millennial-scale climate oscillations during the past 20,000 years. We conclude the following.

1) Surface ocean changes are essentially coincident with the Bølling-Allerød and Younger-Dryas climate oscillations observed in Greenland and the North Atlantic. This finding supports the concept of atmospheric transmission of climate signals between oceans in the Northern Hemisphere. Significant cooling of North Pacific surface waters also occurred in mid-Holocene time, and this event may be part of a widespread phenomenon in the high-latitude regions of the Northern Hemisphere.

2) Organic carbon contents of northeast Pacific sediments suggest that high export productivity was

associated with warm events. This enhanced organic flux probably contributed to depletion of oxygen along the margin of California, and could account for oxic/anoxic oscillations observed there near 400-m water depth, aligned with rapid climatic events observed in Greenland. Although we can not exclude the possibility of variations in thermocline ventilation, major changes in North Pacific Intermediate Water are not required to explain variations in the intensity of the oxygen minimum zone.

3) Benthic foraminiferal $\delta^{13}C$ and ^{14}C data from 980 m depth suggest that higher ventilation (either faster formation or greater gas exchange) of lower intermediate waters occurred during millennial-scale warm intervals, mirroring the Bølling-Allerød and Younger-Dryas climate oscillations observed in Greenland and the North Atlantic. As with the surface water tracers, atmospheric transmission of climate changes within the Northern Hemisphere is supported, but a tentative conclusion that higher intermediate water formation was associated with North Pacific warming suggests that increases in salinity would be required to compensate for effects of warming on water density. We speculate that a mode of circulation with enhanced formation of NPIW during warm events may be self-sustaining and may contribute to the observed range of temperature oscillations in the region.

4) In the deep North Pacific (2700 m), benthic foraminiferal $\delta^{13}C$ and ^{14}C suggest a ventilation event during deglaciation (either faster formation or greater gas exchange) that coincides with the Antarctic Cold Reversal in the Byrd Ice Core. Such a connection, if confirmed at additional sites with firm chronologic constraints, would support the concept of enhanced formation of Antarctic Bottom Water associated with cooling in the Southern Ocean.

5) Benthic foraminiferal $\delta^{18}O$ data from the deep Pacific, compared with available sea level data, suggest that warming of the deep ocean preceded major deglaciation and sea level rise. This warming may be linked to early warming in Antarctica.

6) Our findings of millennial-scale events in the Northeast Pacific, with a range of apparent timings in different proxies from the same sediment core samples, are important because they may reveal dynamic processes in a chain of events leading to natural climate oscillations at millennial and longer scales. The earliest changes appear to be in the deep sea, perhaps associated with events in Antarctica.

7) Research on millennial-scale climate changes in the Pacific region is in its infancy relative to the more heavily studied North Atlantic region. Limits to our findings come from possible chronologic errors and the difficulty in getting good high-resolution records from North Pacific sediments, in which carbonate fossils are relatively rare. To resolve some of these issues in the Pacific, arrays of high-sedimentation rate sites with well-constrained chronologies and a rich array of paleoclimatic proxies are needed.

REFERENCES

Alley, R.B., and P.U. Clark, The deglaciation of the Northern Hemisphere: A global perspective, *Ann. Rev. Earth Planet. Sci., 27,* 149-182, 1999.

Alley, R.B., D.A. Meese, C.A. Shuman, A.J. Gow, K.C. Taylor, P.M. Grootes, J.W.C. White, M. Ram, E.D. Waddinton, P.A. Mayewski, and G.A. Zielinski, Abrupt increase in Greenland snow accumulation at the end of the Younger Dryas event, *Nature, 362,* 527-529, 1993.

Bard, E., Geochemical and geophysical implications of the radiocarbon calibration, *Geochim. Cosmochim. Acta, 62,* 2025-2038, 1998.

Behl, R.J. and J.P. Kennett, Brief interstadial events in the Santa Barbara Basin, NE Pacific, during the past 60 kyr, *Nature, 379,* 243-246, 1996.

Bender, M.L., B. Malize, J. Orchardo, T. Sowers and J. Jouzel, High precision correlations of Greenland and Antarctic ice core records over the last 100 kyr, in *Mechanisms of Millennial Scale Global Climate Change,* edited by P.U. Clark, R.S. Webb, and L.D. Keigwin, AGU, Washington DC, (in press 1999).

Blunier, T., J. Chappellaz, J. Schwander, A. Dällenbach, B. Stauffer, T.F. Stocker, D. Raynaud, J. Jouzel, H.B. Clausen, C.U. Hammer, and S.J. Johnsen, Asynchrony of Antarctic and Greenland climate change during the last glacial period, *Nature, 394,* 739-743, 1998.

Bond, G., W. Broecker, S. Johnsen, J. McManus, L. Labeyrie, J. Jouzel, and G. Bonani, Correlations between climate records from North Atlantic sediment and Greenland ice, *Nature, 365,* 143-147, 1993.

Bond, G. and R. Lotti, Iceberg discharges into the North Atlantic on millennial time scales during the last glaciation, *Science, 267,* 1005-1010, 1995.

Broecker, W.S., Chaotic climate, *Sci. Am.,* November, 62-68, 1995.

Broecker, W.S., Paleocean circulation during the last deglaciation: A bipolar seesaw? *Paleoceanography, 13,* 119-121, 1998.

Broecker, W.S. and E. Maier-Reimer, The influence of air and sea exchange on the carbon isotope distribution in the sea, *Global Biogeochem. Cycles, 6,* 315-320, 1992.

Broecker, W.S., A.C. Mix, M. Andree, and H. Oeschger, Radiocarbon measurements on coexisting benthic and planktic foraminifera shells: Potential for reconstructing ocean ventilation times over the past 20,000 years, *Nuclear Instruments and Methods in Physics Research,* B5, 331-339, 1984.

Broecker, W.S., T. Takahashi, and T. Takahashi, Sources and flow patterns of deep-ocean waters as deduced from potential temperature, salinity, and initial phosphate concentration, *J. Geophys. Res.* 90, 6925-6939, 1985.

Burke, R.M. and P.W. Birkeland, Holocene glaciation in the mountain ranges of the western United States, in *Late*

Quaternary Environments of the United States, edited by H.E. Wright, v.1, pp. 3-11, Univ. Minnesota Press, Minneapolis, MN, 1983.

Campin, J.-M., T. Fichefet, and J.-C. Duplessy, Problems with using radiocarbon to infer ocean ventilation rates for past and present climates, *Earth Planet. Sci. Lett.*, 165, 17-24, 1999.

Cannariato, K.G., J.P. Kennett, and R.J. Behl, Biotic response to late Quaternary rapid switches in Santa Barbara Basin: Ecological and evolutionary implications, *Geology*, 27, 63-66, 1999.

Charles, C.D., J. Lynch-Stieglitz, U.S. Ninnemann, and R.G. Fairbanks, Climate connections between the hemisphere revealed by deep sea sediment core / ice core correlations, *Earth Planet. Sci. Lett.*, 142, 19-27, 1996.

Clark, P.U., R.B. Alley, L.D. Keigwin, J.M. Licciardi, S.J. Johnsen, and H. Wang, Origin of the first global meltwater pulse following the last glacial maximum, *Paleoceanography*, 11, 563-577, 1996.

Clark, P.U. and P.J. Bartlein, Correlations of late Pleistocene glaciation in the western United States with North Atlantic Heinrich events, *Geology*, 23, 483-486, 1995.

Curry, W., J.-C. Duplessy, L.D. Labeyrie, and N.J. Shackleton, Changes in the distribution of $\delta^{13}C$ of deep water ΣCO_2 between the last glaciation and the Holocene. *Paleoceanography*, 3, 317-341, 1988.

Curry, W.B., and D.W. Oppo, Synchronous, high-frequency oscillations in tropical sea surface temperatures and North Atlantic Deep Water production during the last glacial cycle, *Paleoceanography*, 12, 1-14, 1997.

Dansgaard, W., S.J. Johnsen, H.G. Clausen, and C.C. Langway, Jr., Climatic record revealed by the Camp Century ice core, in *The Late Cenozoic Glacial Ages*, edited by K.K. Turekian, pp. 37-56, Yale Univ. Press, New Haven, CT, 1971.

Davis, P.T., Holocene glacier fluctuations in the American cordillera, *Quat. Sci. Rev.*, 7, 129-157, 1988.

Doose, H., F.G. Prahl, and M.W. Lyle, Biomarker temperature estimates for modern and last glacial surface waters of the California Current system between 33° and 42° N, *Paleoceanography*, 12, 615-622, 1997.

Edwards, R.L., J.W. Beck, G.S. Burr, D.J. Donahue, J.M.A. Chappell, A.L. Bloom, E.R.M. Druffel, and F.W. Taylor, A large drop in atmospheric $^{14}C/^{12}C$ and reduced melting in the Younger Dryas, documented with ^{230}Th ages of corals, *Science*, 260, 962-968, 1993.

Fairbanks, R.G., A 17,000-year glacio-eustatic sea level record: influence of glacial melting rates on the Younger Dryas event and deep-ocean circulation, *Nature*, 342, 637-642, 1989.

Fairbanks, R.G. and R.K. Matthews, The marine oxygen isotope record in Pleistocene coral, Barbados, West Indies, *Quat. Res.*, 10, 181-196, 1978.

Freeland, H.J., A.S. Bychkov, FF.Whitney, C. Taylor, C.S. Wong, and G.I Yurasov, WOCE section P1W in the Sea of Okhotsk 1: Oceanographic data description, *J. Geophys. Res.*, 103, 15,613-15,623, 1998.

Gardner, J.V., W.E. Dean, P. Dartnell, Biogenic sedimentation beneath the California Current system for the past 30 kyr and its paleoceanographic significance, *Paleoceanography*, 12, 207-225, 1997.

Grootes, P.M., M. Stuiver, J.W.C. White, S.J. Johnsen, and J. Jouzel, Comparison of oxygen isotope records from the GISP2 and GRIP Greenland ice cores, *Nature*, 366, 552-554, 1993.

Harris, S.E. and A.C. Mix, Pleistocene precipitation balance in the Amazon Basin recorded in deep-sea sediments, *Quat. Res.*, 51, 14-26, 1999.

Harris, S.E., A.C. Mix, and T. King, Biogenic and terrigenous sedimentation at Ceara Rise, western tropical Atlantic, supports Plio-Pleistocene deep-water linkage between hemispheres, in *Proceedings of the Ocean Drilling Program, Scientific Results*, v. 154, edited by N.J. Shackleton, W. Curry, and C. Richter, pp. 331-348, College Station, TX (ODP), 1997.

Hendy, I.L. and J. P. Kennett, Latest Quaternary North Pacific surface-water responses imply atmosphere-driven climate instability, *Geology*, 27, 291-294, 1999.

Heusser, C.J., L.E. Heusser, and S.S. Streeter, Quaternary temperatures and precipitation for the Northwest coast of North America, *Nature*, 286, 702-704, 1980.

Hood, R., M. Abbott, A. Huyer, and P.M. Kosro, Surface patterns in temperature, flow, phytoplankton biomass, and species composition in the coastal transition zone off Northern California, *J. Geophys. Res.*, 95, 18,081-18,094, 1990.

Hostetler, S.W., P.U. Clark, P.J. Bartlein, A.C. Mix, and N.J. Pisias, Atmospheric transmission of North Atlantic Heinrich events, *J. Geophys. Res.*, 104, 3947-3952, 1999.

Hughen, K.A., J.T. Overpeck, S.J. Lehman, M. Kashgarian, J. Southon, L.C. Peterson, R. Alley, and D.M. Sigman, Deglacial changes in ocean circulation from an extended radiocarbon calibration, *Nature*, 391, 65-68, 1998.

Huyer, A., Coastal upwelling in the California Current System. *Prog. Oceanography*, 12, 259-284, 1983.

Imbrie, J., A. McIntyre, and A.C. Mix, Oceanic response to orbital forcing in the late Quaternary: Observational and Experimental Strategies, in *Climate and Geosciences*, edited by A. Berger, S. Schneider, and J.-C. Duplessy, pp. 121-164, Kluwer Academic, Dordrecht, 1989.

Ingram, B.L. and J.P. Kennett, Radiocarbon chronology and planktonic-benthic foraminiferal ^{14}C age differences in Santa Barbara Basin sediments, Hole 893A, in *Proceedings of the Ocean Drilling Program, Scientific Results*, v. 146, edited by J.P. Kennett, J.G. Baldauf, and M. Lyle, pp. 19-27, College Station, TX (ODP), 1996.

Johnsen, S.J., W. Dansgaard, H.B. Claussen, and C.C. Langway, Oxygen isotope profiles through the Antarctic and Greenland ice sheets, *Nature*, 235, 429-434, 1972.

Johnson, K.S., F.P. Chavez, and G.E. Friederich, Continental-shelf sediment as a primary source of iron for coastal phytoplankton, *Nature*, 398, 697-700, 1999.

Keigwin, L.D., Glacial-age hydrography of the far northwest Pacific Ocean, *Paleoceanography*, 13, 323-339, 1998.

Keigwin, L.D. and G.A. Jones, Deglacial climatic oscillations in the Gulf of California, *Paleoceanography*, 5, 1009-1023, 1990.

Kennett, J.P. and B.L Ingram, A 20,000-year record of ocean circulation and climate change from the Santa Barbara Basin, *Nature*, 377, 510-514, 1995.

Kerwin, M.W., J.T. Overpeck, R.S. Webb, A. DeVernal, D.H. Rind, and R.J. Healy, The role of oceanic forcing in mid-Holocene Northern Hemisphere climate change, *Paleoceanography*, 14, 200-210, 1999.

Kipp, N.G., New transfer function for estimating past sea-surface conditions from sea-bed distribution of planktonic foraminiferal assemblages in the North Atlantic, in *Investigation of Late Quaternary Paleoceanography and Paleoclimatology*, edited by R.M. Cline, and J.D. Hays, Memoir 145, pp. 3-42, Geol. Soc. America, Boulder, CO, 1976.

Kotilainen, A.T., and N.J. Shackleton, Rapid climate variability in the North Pacific Ocean during the past 95,000 years, *Nature*, 377, 323-326, 1995.

Kroopnick, P.M., The distribution of ^{13}C of TCO$_2$ in the world oceans, *Deep-Sea Res.*, 32, 57-84, 1985.

Lowell, T.V., C.J. Heusser, B.G. Andersen, P.I. Moreno, A. Hauser, L.E. Heusser, C. Schluchter, D.R. Marchant, and G.H. Denton, Interhemispheric correlation of late Pleistocene glacial events, *Science*, 269, 1541-1549, 1995.

Lund, D.C. and A.C. Mix, Millennial-scale deep water oscillations: Reflections of the North Atlantic in the deep Pacific from 10 to 60 ka, *Paleoceanography*, 13, 10-19, 1998.

Lyle, M., I. Koizumi, C. Richter, and the shipboard scientific party, *Proceedings of the Ocean Drilling Program, Initial Reports*, (part 1), 167, 0-495pp, College Station, TX (ODP), 1997.

Lyle, M., A. Mix, C. Ravelo, D. Andreasen, L. Heusser, A. Olivarez, Kyr-scale CaCO$_3$ and C$_{org}$ events along the northern and central California margin: Stratigraphy and origins, *Proceedings of the Ocean Drilling Program, Scientific Results*, 167, edited by M. Lyle, I. Koizumi, and C. Richter, College Station, TX (ODP), in press 1999.

Lyle, M., R. Zahn, F. Prahl, J. Dymond, R. Collier, N. Pisias, and E. Suess, Paleoproductivity and carbon burial across the California Current: The multitracers transect, 42°N, *Paleoceanography*, 7, 251-272, 1992.

Lynn, R.J. and J.J. Simpson, The California Current System: The Seasonal variability of its physical characteristics, *J. Geophys. Res.*, 92, 12947-12966, 1987

MacAyeal, D.R., Growth/Purge oscillations of the Laurentide ice sheet as a cause of the North Atlantic's Heinrich events. *Paleoceanography*, 8, 775-784, 1993.

Manabe, S., and R.J. Stouffer, Two stable equilibria of a coupled ocean-atmosphere model, *J. Climate*, 1, 841-866, 1988.

Mantyla, A.W., and J.L. Reid, Abyssal characteristics of the world ocean waters, *Deep-Sea Res.*, 30, 805-833, 1983.

Mathewes, R.W. and L.E. Heusser, A 10,000 year palynological record of temperature and precipitation trends in southwestern British Columbia, *Can. J. Bot.*, 59, 707-710, 1981.

Mikolajewicz, U., T.J. Crowley, A, Schiller, and R. Voss, Modeling teleconnections between the North Atlantic and North Pacific during the Younger Dryas, *Nature*, 387, 384-387, 1997.

Mix, A.C., S.E. Harris and T. Janecek,. Estimating lithology from nonintrusive reflectance spectra: ODP Leg 138, in *Proceedings of the Ocean Drilling Program, Scientific Results*, 138, edited by N.G. Pisias, L. Mayer, T. Janecek, A. Palmer-Julson, and T.H. van Andel, pp. 413-428, College Station, TX (ODP), 1995.

Mix, A.C., N.G. Pisias, W. Rugh, S. Veirs, Leg 138 Shipboard Sedimentologists, and the Leg 138 Scientific Party, Color reflectance spectroscopy: A tool for rapid characterization of deep-sea sediments. In: *Proceedings of the Ocean Drilling Program, Initial Repts*, 138 (volume 1), edited by L. Mayer, N. Pisias, and T. Janecek, pp. 67-77, College Station, TX, (ODP), 1992.

Ninnemann, U., and C.D. Charles, Regional differences in Quaternary Subantarctic nutrient cycling: Link to intermediate and deep water ventilation, *Paleoceanography* 12, 560-567, 1997.

Oppo, D.W. and S.J. Lehman, Suborbital timescale variability of North Atlantic Deep Water during the past 200,000 years, *Paleoceanography*, 10, 901-910, 1995.

Ortiz, J., A. Mix, S. Harris, and S. O'Connell, Diffuse spectral reflectance as a proxy for percent carbonate content in North Atlantic sediments. *Paleoceanography*. 14, 171-186, 1999.

Ortiz, J.D., A.C. Mix, S. Hostetler, and M. Kashgarian, The California Current of the last glacial maximum: Reconstruction at 42°N based on multiple proxies, *Paleoceanography*, 12, 191-205, 1997.

Parker, F., Planktonic foraminiferal species in Pacific sediments, *Micropaleontology*, 8, 219-254, 1962.

Peteet, D., A. Del Genio, and K.-W. Lo, Sensitivity of Northern Hemisphere air temperatures and snow expansion to North Pacific sea surface temperatures in the Goddard Institute for Space Studies general circulation model. *J. Geophys. Res.* 102, 23,781-23,791, 1997.

Pisias, N.G., Model for paleoceanographic reconstructions of the California Current during the last 8000 years. *Quat. Res.*, 11, 373-386, 1979.

Pisias, N., Sancetta, C., and Dauphin, P., Spectral analysis of late Pleistocene-Holocene sediments, *Quat. Res.*, 3, 3-9, 1973.

Porter, S.C. and Z. An, Correlation between climate events in the North Atlantic and China during the last glaciation, *Nature* 375, 305-308, 1995.

Rahmstorf, S., Bifurcations of the Atlantic thermohaline circulation in response to changes in the hydrological cycle, *Nature*, 378, 145-149, 1995.

Reid, J.L., Jr., *Intermediate waters of the Pacific Ocean*, 85 pp., Johns Hopkins Press, Baltimore, MD, 1965.

Robinson, S.W.and G. Thompson, Radiocarbon corrections for marine shell dates with application to southern Pacific Northwest Coast prehistory, *Syesis*, 14, 45-57, 1981.

Sabin, A.L. and N.G. Pisias, Sea surface temperature changes in the Northeast Pacific Ocean during the past 20,000 years and their relationship to climatic change in Northwestern North America, *Quat. Res.*, 46, 48-61, 1996.

Saito, T., P.R. Thompson and D. Breger, *Systematic Index of Recent and Pleistocene Planktonic Foraminifera*, Univ. Tokyo Press, Tokyo, Japan, 1981.

Sancetta, C., M. Lyle, L. Heusser, R. Zahn, and J.P. Bradbury, Late-glacial to Holocene changes in winds, upwelling, and seasonal production of the northern California Current system, *Quat. Res.*, 38, 359-370, 1992.

Schrag, D.P., G. Hampt, and D.W. Murray, The temperature and oxygen isotopic composition of the glacial ocean, *Science*, 272, 1930-1932, 1996.

Smith, A.B., Living planktonic foraminifera collected along an east-west traverse in the North Pacific, *Contrib. Cushman Foundation for. Foraminiferal Research*, 15, 131-134,1964.

Southon, J.R., D.E. Nelson, and J.S. Vogel, A record of past ocean-atmosphere radiocarbon differences from the northeast Pacific, *Paleoceanography*, 5, 197-206, 1990.

Stuiver, M. and P.J. Reimer, Extended ^{14}C database and revised CALIB radiocarbon calibration program, *Radiocarbon*, 35, 215-230, 1993.

Stuiver, M., P.J. Reimer, E. Bard, J.W. Beck, G.S. Burr, K.A. Hughen, B. Kromer, F.G. McCormac, J. vanderPlicht, and M. Spurk, INTCAL98 radiocarbon age calibration, 24,000-0 cal BP, *Radiocarbon*, 40, 1041-1083, 1998.

Takeda, S., Influence of iron availability on nutrient consumption ratio of diatoms in oceanic waters, *Nature* 393, 774-777, 1998.

Talley, L., Distribution and formation of the North Pacific Intermediate Water, *J. Phys. Ocean.*, 23, 517-537, 1993.

Thunell, R. and P.G. Mortyn, Glacial climate instability in the northeast Pacific Ocean, *Nature*, 376, 504-506, 1995.

Toggweiler, J.R., K. Dixon, and K. Bryan, Simulations of radiocarbon in a coarse-resolution world ocean model, 1, steady state prebomb distributions, *J. Geophys. Res.*, 94, 8217-8242, 1989.

Toggweiler, J.R., and B. Samuels, Effect of Drake Passage on the global thermohaline circulation, *Deep-Sea Res.* 42, 477-500, 1993.

van Geen, A., R.G. Fairbanks, P. Dartnell, M. McGann, J.V. Gardner, and M. Kashgarian, Ventilation changes in the northeast Pacific during the last deglaciation, *Paleoceanography*, 11, 519-528, 1997.

van Scoy, K.A., D.B. Olson, and R.A. Fine, Ventilation of the North Pacific Intermediate waters: The role of the Alaskan Gyre, *J. Geophys. Res.*, 96, 16,801-16,810, 1991.

Warren, B.A., Why is no deep water formed in the North Pacific? *J. Mar. Res.*, 41, 327-347, 1983.

Yamanaka, G., Y. Kitamura, and M. Endoh, Formation of North Pacific Intermediate Water in Meteorological Research Institute ocean general circulation model 1: Subgrid-scale mixing and marginal sea fresh water, *J. Geophys. Res.*, 103, 30,885-30,903, 1998.

Zahn, R., T.F. Pedersen, B.D. Bornhold, and A.C. Mix, Water mass conversion in the glacial subarctic Pacific (54°N, 148°W): Physical constraints and the benthic-planktonic stable isotope record, *Paleoceanography*, 6, 543-560, 1991.

Zahn, R., K. Winn, and M. Sarnthein, Benthic foraminiferal δ^{13}C and accumulation rates of organic carbon, Uvigerina peregrina group and Cibicidoides wuellerstorfi, *Paleoceanography*, 6, 543-560, 1986.

P. Bodén, Dept. of Geology and Geochemistry, Stockholm University, S-106 91, Stockholm, Sweden (per.boden@geo.su.se)

L. Bornmalm, Dept. of Marine Geology, Göteborg University, Box 460, S-403 Göteborg, Sweden (lennart@gvc.gu.se)

M. Lyle, CGISS, Boise State University, Boise, ID 83725 (mlyle@kihei.boisestate.edu)

D.C. Lund, Kennedy School of Government, 79 JFK Street, Harvard University, Cambridge, MA 02138 (dave_lund@harvard.edu)

A.C. Mix, College of Oceanic and Atmospheric Sciences, Oregon State University, Corvallis, OR 97331 (mix@oce.orst.edu)

J. Pike, Department of Earth Sciences, Cardiff University, PO Box 914, Cardiff, CF1 3YE, UK (pikej@cardiff.ac.uk)

N.G. Pisias, College of Oceanic and Atmospheric Sciences, Oregon State University, Corvallis, OR 97331 (pisias@oce.orst.edu)